



HAL
open science

Development and characterization of composite films based on chitosan and collagenous proteins from bluefin tuna: application for peeled shrimp preservation

Youssra Ben Azaza, Marwa Hamdi, Christophe Charmette, Arie van der Lee, Mourad Jridi, Suming Li, Moncef Nasri, Rim Nasri

► To cite this version:

Youssra Ben Azaza, Marwa Hamdi, Christophe Charmette, Arie van der Lee, Mourad Jridi, et al.. Development and characterization of composite films based on chitosan and collagenous proteins from bluefin tuna: application for peeled shrimp preservation. *Cellulose*, 2023, 30 (1), pp.373-395. 10.1007/s10570-022-04893-z . hal-04055778

HAL Id: hal-04055778

<https://hal.umontpellier.fr/hal-04055778v1>

Submitted on 7 Sep 2023

HAL is a multi-disciplinary open access archive for the deposit and dissemination of scientific research documents, whether they are published or not. The documents may come from teaching and research institutions in France or abroad, or from public or private research centers.

L'archive ouverte pluridisciplinaire **HAL**, est destinée au dépôt et à la diffusion de documents scientifiques de niveau recherche, publiés ou non, émanant des établissements d'enseignement et de recherche français ou étrangers, des laboratoires publics ou privés.

1 **Development and characterization of composite films based on chitosan and**
2 **collagenous protein from bluefin tuna: Application for peeled shrimp**
3 **preservation**

4
5 Youssra Ben Azaza*¹, Marwa Hamdi¹, Christophe Charmette², Arie van der Lee², Mourad
6 Jridi^{1,3}, Suming Li², Moncef Nasri¹, Rim Nasri^{1,4}

7 1 Laboratory of Enzyme Engineering and Microbiology, University of Sfax, National Engineering
8 School of Sfax, P.O.B. 1173-3038 Sfax, Tunisia

9 2 Institut Européen des Membranes, IEM, UMR 5635, Univ Montpellier, ENSCM, CNRS, Montpellier,
10 France.

11 3 Higher Institute of Biotechnology of Beja, University of Jendouba, Beja, Tunisia

12 4 Higher Institute of Biotechnology of Monastir, P.O.B. 5000, University of Monastir, Monastir, Tunisia

13
14
15
16
17 * Corresponding author : Laboratory of Enzyme Engineering and Microbiology, University of Sfax,
18 National Engineering School of Sfax, P.O.B. 1173, 3038, Sfax, Tunisia.

19 E-mail address: youssrabenazaza@gmail.com (Y. Ben Azaza).
20
21
22
23
24
25
26
27
28
29
30
31
32
33
34
35
36
37

38 **Abstract**

39 In the current study, composite films based on blue crab chitosan (Cs) and bluefin tuna
40 collagenous proteins (BTCP) were prepared and characterized. Composite films were assessed
41 for their physicochemical, barrier (water vapor and UV), structural, crystallinity, thermal,
42 mechanical and antioxidant properties. FTIR analysis showed an increase of hydrogen bonding
43 formation between polymers with the increase of BTCP content. Additionally, the addition of
44 BTCP to the Cs solution at a volume ratio of 10:90, consequently forming the Cs90-10BTCP
45 film, improved the water vapor permeability and UV barrier capability of the composite films
46 compared to the chitosan film. Interestingly, the incorporation of BTCP improved significantly
47 the antioxidant activity of composite films, allowing them to be successively used as bioactive
48 packaging materials. The ability of Cs-BTCP film solutions as a coating for shrimp preservation
49 was also investigated. The Cs90-10BTCP film solution showed better preservative effect on
50 shrimps in terms of preventing the lipid peroxidation and delaying the growth of spoilage
51 microorganisms. Hence, these findings suggested that the Cs-BTCP coating preserved the
52 shrimps throughout the refrigerated storage period.

53 **Keywords:** Composite films; Shrimp coating; Postharvest shelf life.

54

55

56

57

58

59

60

61

62

63

64

65

66

67

68 **1. Introduction**

69 The growth of the world population, leads to a scarcity of biological resources and an
70 increasing degradation of the environment, hence the need for innovation in the food sector

71 (Kaanane and Mkaem 2020). To minimize food loss and waste in the fish value chains and, at
72 the same time, improve fish waste management strategies, several methods can be used to
73 convert by-products into value added products: animal feed ingredients (fishmeal and fish oil),
74 dietetic products (chitosan), pharmaceuticals (omega-3 oils) and constituents in other industrial
75 processes (Al Khawli et al. 2019; Caruso et al. 2020).

76 The valorization of marine by-products should be a necessity to guarantee global food
77 security and satisfy of the growing demand for fishery products (Rudovica et al. 2021). Marine
78 by-products (viscera, heads, bones, cartilages, skin, scales, shells, damaged fish), produced by
79 marine processing industries (Hamed et al. 2016), are a good alternative to high-value products
80 (Galiano et al. 2018).

81 Crustacean products represent a valuable source of proteins, chitin (Hajji et al. 2014),
82 minerals, carotenoids (Hamdi et al. 2019), flavors, nutritive components and enzymes (Affes et
83 al. 2019). Therefore, making use of such waste was due to their biological and economical
84 values (Ozogul et al. 2018). The seafood industry generates about 2,000 tons of chitosan
85 annually, whose main source of extraction is from crustacean exoskeletons (Muñoz et al. 2018;
86 Santos et al. 2020).

87 In this context, chitosan, a natural polymer obtained from blue crab shell, plays an
88 important role due to its outstanding characteristics such as nontoxicity, low allergenicity,
89 biocompatibility, and biodegradability. It has been evaluated as a biomaterial for various
90 applications (Aranaz et al. 2021). Chitosan, consisting of units of D-glucosamine and N-acetyl-
91 D-glucosamine, linked by β -1,4-glycosidic bonds, is a cationic polysaccharide obtained by
92 deacetylation of chitin (Hamdi et al. 2020). The cationic nature of chitosan allows it to form
93 electrostatic complexes or multilayer structures with other negatively charged natural polymers.

94 Chitosan is known as an excellent film forming polymer (Wang et al. 2020). The chitosan
95 films have been extensively studied for their good barrier properties against oxygen, water and
96 lights (Kittur et al. 1998; Melro et al. 2020). Despite these advantages, Cs-based films present
97 some drawbacks in food packaging, such as brittleness, poor mechanical resistance, low thermal
98 stability, and sensitivity to moisture (Aider 2010; Yuan et al. 2021).

99 Therefore, to enhance the performance of the Cs-based film, the blending strategy with
100 other biopolymers would be an alternative approach to improve the film properties (Zhang et
101 al. 2020; Li et al. 2020). Always, films made by mixing polymers usually have enhanced
102 physical and mechanical properties compared to films made of individual components.

103 Fish protein isolates can be prepared from protein isolation process of fish by-product.
104 The use of protein isolate has already been used not only as food additive but also as film-

105 forming materials (Valdivia-López et al. 2016; Mihalca et al. 2021). However, fish protein
106 isolates-based films have certainly poor properties. Thus, many studies have been made to show
107 the effect of blending marine protein isolates with chitosan on improving different properties
108 of Cs-based film (Zhang et al. 2019; Azaza et al. 2022).

109 The composite films, with improved properties, are currently attracting increasing interest
110 in the development of packaging materials for food preservation. The potential of edible
111 coatings is to improve the quality of food products by delaying lipid oxidation, preventing loss
112 of protein functionality and reducing bacterial growth (Barlow and Morgan 2013).

113 In this study, the head and cartilage of bluefin tuna (*Thunnus thynnus*) were used as a by-
114 product model of fish processing and were valued by the protein isolation process, which is
115 currently the most processed axis for producing biopolymers. This approach involves
116 solubilizing/precipitating of the collagenous protein at low pH separating the soluble proteins.
117 It could be an excellent and viable practice to effectively value this new biomass. As a natural
118 protein, collagenous protein, extracted from by-products of bluefin tuna (*T. thynnus*), was used
119 in polymer-based films due to its functional and antioxidant properties. Cs and BTCP can be
120 used as a potential biological matrix for the development of composite film combined at
121 different ratios, with interesting properties, widely used for various applications. Additionally,
122 this study was carried out to investigate the effect of Cs-BTCP coating on the chemical,
123 microbiological and lipid oxidative changes of shrimp during refrigerated storage was
124 evaluated. This research is of special importance in the sectors of the blue and circular economy
125 and the sustainable use of marine by-products. For this reason, this study aims to valorize these
126 by-products, which can be used as a potential biological matrix for the extraction of bioactive
127 substances with high added value exploitable in several fields.

128 **2. Materials and methods**

129 **2.1. Materials**

130 Blue crab samples were obtained under fresh conditions from a fishery market located at
131 Sfax City, Tunisia.

132 Bluefin tuna by-products were collected from the "The Sultan" tuna fishery in Sfax City,
133 Tunisia. Glycerol and acetic acid were purchased from Sigma-Aldrich. DPPH (2, 2-diphenyl-
134 1-picrylhydrazyl), ferrozine (3-(2-Pyridyl)-5,6-diphenyl-1,2,4-triazine), ferrous chloride,
135 ferrous ion, α -tocopherol, potassium ferricyanide, trichloroacetic acid (TCA), sodium chloride
136 (NaCl), ammonium thiocyanate, Tris, butylated hydroxytoluene (BHT) and 2/thiobarbituric
137 acid (TBA) were procured from Sigma Chemical Co. (St. Louis, MO, USA).

138 Hexane, hydrochloric acid (HCl), chloroform and methanol of reagent grade were
139 purchased from Sigma Chemical Co.

140 **2.2. Preparation of blue crab chitosan**

141 Chitosan was extracted from blue crab (*P. segnis*) shells as described by Azaza et al.
142 (2022). Blue crab shells were carefully separated and washed with tap water to remove
143 impurities and cooked for 20 min at 90 °C. Then, the cooked shells were dried at room
144 temperature and powdered in a Moulinex® blender. In the Cs preparation process, there must
145 be at least two distinct steps, namely a demineralization (mineral removal) step, performed
146 chemically in a reactor under agitation and in a solution of HCl (0,55 M) at a ratio of 1/10 (m/v),
147 using three repeated acid baths, for a duration of 30 min each bath and a deproteinization step
148 (protein removal), was carried out using Purafect® for 3 hours with an enzyme/substrate ratio
149 of 5 U/mg protein and under optimal enzyme conditions (pH 10.0 and temperature 50 °C).
150 Finally, the conversion of chitin to chitosan was realized with the treatment of with 12.5 M
151 NaOH at a w/v ratio of 1/10 to 140 °C. After filtration, the residue was washed with distilled
152 water until the pH was neutral, and the crude chitosan was dried at 50 °C for overnight.

153 **2.3. Characteristics of blue crab chitosan**

154 The degree of deacetylation (DD) of Cs was determined by using the direct titration
155 method as described by Hamdi et al. (2018). Briefly, chitosan samples (0.1 g) were dissolved
156 in 25 mL of 0.06 M HCl for 1 h at room temperature. Before being titrated with a 0.1 M NaOH
157 to pH 3.75 under constant stirring, the solutions were diluted to 50 ml with distilled water. The
158 volume of NaOH at pH 3.75 was acquired and recorded. Titration was continued to pH 8 and
159 the total volume of NaOH (0.1 M) was recorded. The degree of deacetylation (DD) was, then,
160 calculated using the following equations:

$$161 \quad DD (\%) = 161.16 \times (V2 - V1) \times N / W1 \quad \text{Eq (1)}$$

162 where, 161.16 is the mass (g mol⁻¹) of chitosan monomer ; V1 and V2 are the volumes required
163 at pH 3.75 and pH 8.0, respectively, of NaOH solution used (in L); N is the strength of the
164 NaOH solution (0.1 M) and W1 is the mass (in g) of sample after correction for moisture. The
165 degree of deacetylation (DD) of the samples was determined in triplicate.

166 Steric Exclusion Chromatography (SEC) was performed using multi-detector equipment
167 with a differential refractometer, a multiangle laser light scattering detector and a viscometer
168 from WYATT Technology (DAWN DSP-F). Acetic acid 0.3 M/sodium acetate 0.2 M
169 (pH = 4.5) was adopted as solvent (at 25 ± 2 °C). TSK Gel GMPWXL column type was used
170 and a flow of 0.4 ml/min was adopted. The increment of refractive index dn/dc was 0.190

171 (Hamdi et al. 2020). Resulted chromatograms were analyzed with ASTRA 6.1.2 (WYATT
172 Technology) software and weight-average molecular weights (M_w ; g mol^{-1}), were determined.

173 The DD of Cs, estimated by potentiometric titration, was found to be significantly high
174 ($90.39 \pm 1.36 \%$) as mentioned by Hamdi et al. (2018). Further, the average molecular weight
175 of the obtained Cs was estimated to be $115\,000 \text{ g mol}^{-1}$, based on the size exclusion
176 chromatography (SEC) analysis (Hamdi et al. 2020).

177 **2.4. Preparation of bluefin tuna collagenous proteins**

178 The extraction of collagenous proteins was carried out as follows: first of all, the bluefin
179 tuna by-products (equal weight ratio of head and cartilage) were grounded and then mixed with
180 distilled water at a ratio of 1:10 (w/v) using an Ultra-turrax® apparatus (IKA, T18 basic).
181 Afterward, the pH of the mixture was adjusted to 5.0 using 1 M HCl solution, and the mixture
182 was kept under constant stirring at $50 \text{ }^\circ\text{C}$ overnight. The soluble collagenous proteins were
183 recovered in the supernatant after centrifugation at 6000 rpm for 30 min. Finally, the pH of the
184 supernatant was adjusted to 7.0 using 2 M NaOH solution, and the bluefin tuna collagenous
185 proteins (BTCP) were spray-dried using an atomizer (BUCHI B-290, Arch Spray Drying
186 Services, USA).

187 The extraction yield of BTCP was calculated as follows,

$$188 \quad \text{Yield (\%)} = \frac{W}{W_0} \times 100 \quad \text{Eq (2)}$$

189 where W is the weight of dried BTCP (g), and W_0 the wet weight of fresh bluefin tuna by-
190 products (g).

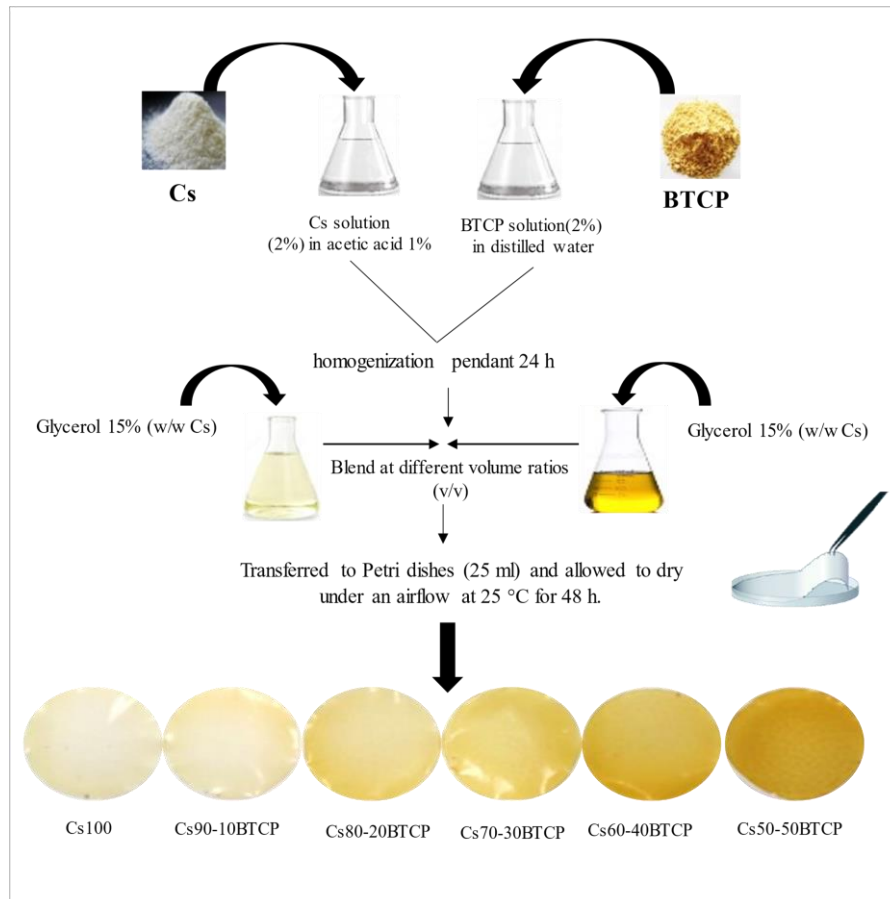
191 **2.5. Chemical analysis of BTCP**

192 The dry matter, moisture, and ash contents of BTCP were determined according to the
193 AOAC standard method (Horwitz 2000). Proteins content of dried BTCP was measured using
194 the Kjeldahl method and the method developed by Lowry et al. (1951). All measurements were
195 performed in triplicate.

196 **2.6. Preparation of Cs-BTCP composite films**

197 Film-forming solutions were prepared as reported in our previous study (Azaza et al.
198 2022), by dissolving Cs (2%; w/v) in 1% (v/v) aqueous acetic acid and BTCP (2%; w/v) in
199 distilled water, under continuous magnetic stirring at room temperature (**Fig. 1**). After complete
200 solubilization, both polymer solutions were filtered to remove insoluble impurities, and then
201 glycerol, as a plasticizer, was added to both solutions at a level of 15% (w/w compared to

202 polymer), respectively. Next, the solutions were blended by mixing under gentle stirring at
 203 different Cs-BTCP volume ratios. The film-forming solutions were poured into Petri dishes (25
 204 ml) and allowed to dry under an air flow at 25 °C for 48 h. The dried Cs/BTCP films were
 205 peeled off carefully and stored at 25 °C and a relative humidity (RH) of 50%, for further
 206 analysis. The obtained composite films were designated as Cs90–10BTCP, Cs80–20BTCP,
 207 Cs70–30BTCP, Cs60–40BTCP and Cs50–50BTCP. Pure chitosan (Cs100) films were prepared
 208 as control.



209

Fig. 1 Preparation scheme of Cs-BTCP composite films

210

211 **2.7. Characterization of Cs-BTCP composite films**

212 *2.7.1. Moisture content and water solubility*

213 Moisture content (MC) was evaluated by drying approximately 100 mg of film samples
 214 in an oven at 105 °C up to constant weight. The weights of films before and after drying were
 215 measured and the MC of films was calculated as follows:

216
$$MC (\%) = \frac{W_0 - W}{W_0} \times 100 \quad \text{Eq (3)}$$

217 where W_0 is the initial film weight (g) and W is the final film dry weight (g). Three replicates
218 of each film were carried out.

219 Water solubility (WS) of Cs-BTCP composite films was assayed as reported by
220 Gennadios et al. (1998) . Briefly, Small pieces of the films (100 mg) were placed in centrifuge
221 tube containing 50 ml distilled water at 25 °C and then shaken for 24 h. After centrifugation
222 (8000 rpm – 15 min), the residual pieces of films were dried at 50 °C for 24 h.
223 The WS was calculated as follows:

$$224 \quad WS (\%) = \frac{[W_0 \times (100 - MC) - W_f]}{[W_0 \times (100 - MC)]} \times 100 \quad \mathbf{Eq (4)}$$

225 where W_0 is the initial film weight (g), W_f is the final dry weight of film (g), and MC is the
226 moisture content of films. All experiments were performed in triplicates.

227 2.7.2. Swelling degree

228 The swelling degree (SD) of Cs-BTCP composite films was determined according to the
229 method reported by Khan and Ranjha, (2014). Film samples (30 mg) were immersed in 10 mL
230 distilled water for 24 h at 25 °C. After incubation, excess water was removed and the films were
231 carefully dried on filter papers and weighed again. Swelling degree was calculated as follows:

$$232 \quad SD (\%) = \frac{W_f - W_i}{W_i} \times 100 \quad \mathbf{Eq (5)}$$

233 where W_i is the initial weight of the film (g) and W_f is the final weight of the swollen film (g).
234 The weight measurements were performed in triplicate

235 2.7.3. Water/vapor permeability (WVP)

236 Water vapor permeability (WVP) was evaluated gravimetrically according to ASTM
237 E96-95 standards. The film samples (75 × 75 mm) were conditioned at 25 °C and 50% RH for
238 a minimum equilibration time of 48 h and thickness was measured for all samples after
239 equilibration. The WVP cup was placed in a humidity chamber (KBF 240 Binder, ODIL,
240 France) maintained at 25 °C and 50% RH. The change in the weight of the cup was measured
241 at regular intervals of 1 h over 10 h. The WVP ($\text{g m}^{-1} \text{s}^{-1} \text{Pa}^{-1}$) was calculated by the following
242 equation:

$$243 \quad WVP = \frac{\Delta w \times e}{A \times \Delta t \times \Delta P} \quad \mathbf{Eq (6)}$$

244 where Δw is the weight variation of the cup (g); e is the film thickness (m); A is the film area
245 exposed to the transfer ($1.39 \times 10^4 \text{ m}^2$); Δt is the time of weight variation (s); $\Delta P = (p_2 - p_1)$ is
246 the vapor partial pressure differential across the film (Pa). All films were measured three times.

247 2.7.4. Light transmission and transparency

248 The Cs-BTCP composite films light transmittance was determined at wavelengths ranged
249 from 200 to 800 nm using UV/visible spectrometer (T70, UV / Vis spectrometer, PG
250 Instruments Ltd., China) as described by Fang et al. (2002). Briefly, films were cut into
251 rectangular samples (1 x 3 cm) and directly attached on the internal side the spectrophotometer.
252 The transparency was determined at 600 nm and calculated as follows:

$$253 \quad \text{Transparency} = \frac{\text{Log}A_{600}}{t} \quad \text{Eq (7)}$$

254 where A_{600} is the film absorbance at 600 nm and t is the film thickness (μm). Measurements
255 were carried out in triplicate.

256 2.7.5. Color properties

257 Film color properties were measured using a colorimeter Konica Minolta CR/5 (Sensing
258 Europe B.V) to obtain parameters L^* (lightness/brightness), a^* (redness/greenness), b^*
259 (yellowness) and ΔE^* (total color difference). The control film (Cs100) was used as a reference
260 for color measurements of the films. The measurements were repeated five times for each
261 sample. The color difference ΔE was calculated by using the following equation:

$$262 \quad \Delta E^* = [(\Delta L^*)^2 + (\Delta a^*)^2 + (\Delta b^*)^2]^{1/2} \quad \text{Eq (8)}$$

263 where ΔL^* , Δa^* and Δb^* are the differences between the corresponding color parameter of
264 the sample and that of the control film.

265 2.7.6. Fourier transform infrared (FTIR) spectroscopy

266 FTIR spectra were recorded on a spectrometer (Agilent Technologies, Carry 630 series)
267 equipped with horizontal attenuated total reflectance (ATR) crystal (diamond/ZnSe) in the
268 wavenumber range from 650 to 4000 cm^{-1} . A total of 32 scans was made per minute at 4 cm^{-1}
269 resolutions. All spectra were smoothed using the OMNIC Spectra software (ThermoFisher
270 Scientific).

271 2.7.7. X-ray diffraction (XRD) analysis

272 The XRD patterns were recorded by a Bruker D5000 ray diffractometer with a radiation
273 source of Cu $K\alpha$. Measurements were made from 7 to 40° at a scanning rate of 1°/min, a voltage

274 of 40 KV and a current of 20 mA. A blank run was done and subtracted subsequently from the
275 sample data.

276 *2.7.8. Thermogravimetric analysis (TGA)*

277 The thermal stability of composite films was conducted by using thermogravimetric
278 analyzer (TGA Q500 High Resolution, TA Instruments). Dynamic scans from 25 to 600 °C
279 were carried out at a constant rate of 20 °C/min under nitrogen flow (40 mL/min). 4 mg of
280 sample were used for each analysis.

281 *2.7.9. Mechanical properties*

282 Tensile strength (TS) and elongation at break (EAB) of film samples were evaluated at
283 25 °C using a rheometer (Physica MCR. Anton Paar. GmbH. France) equipped with a
284 mechanical property measuring geometry. Rectangular samples (4.5 cm × 1.0 cm) were cut
285 from films using a precision standard cutter. After equilibrating films for one week at 25 °C
286 and 50 % RH, the thicknesses were measured. The samples were placed in the extension grips
287 of the testing machine and stretched uniaxially with a deformation rate of 5 mm/min until
288 breaking. Rheoplus software was used for the estimation of TS (MPa) and EAB (%)
289 corresponding to the maximum load and the final extension at break from the stress/strain
290 curves, respectively. The average values of at least six measurements were listed.

291 The thickness of Cs-BTCP composite films was measured using micrometer (Digimatic
292 IP65, Mitutoyo, France); with an accuracy of ± 0.001 mm. Ten random measurements at
293 different positions of each sample were used to determine the thickness of the films. Thickness
294 results were taken into account for mechanical properties and water vapor permeability
295 determination.

296 *2.7.10. In vitro antioxidant activity of films*

297 **2.7.10.1. DPPH free radical-scavenging assay**

298 The DPPH free radical scavenging activity of prepared films was evaluated according to
299 the method of Bersuder et al. (1998), with some modifications. The films were cut into small
300 pieces (m = 10 mg) and immersed in 375 µl of 99.5 % ethanol and 125 µl of 0.02% DPPH (in
301 99.5 % ethanol), as free radicals' source. The mixture was homogenized and incubated for 24
302 h at room temperature (25 °C) in the dark. The reduction of DPPH radicals was measured at
303 517 nm (T70, UV/Vis spectrometer, PG Instruments Ltd., China). Regarding the solutions of
304 BTCP powder, it was the same process used for all film samples. The butylated hydroxyanisole

305 (BHA) was used as a positive control and the anti-radical activity was calculated according to
306 the following equation:

$$307 \quad \text{Radical scavenging activity (\%)} = \frac{[Abs_c + Abs_B - Abs_F]}{Abs_c} \times 100 \quad \text{Eq (9)}$$

308 where Abs_c is the absorbance of the control reaction, Abs_B and Abs_F were the absorbance of
309 the blank and the reaction mixture, respectively. The test was carried out in triplicate.

310 **2.7.10.2. Metal chelating activity**

311 The chelating activity of prepared films towards ferrous ion (Fe²⁺) was studied as reported
312 by Decker and Welch, (1990), with some modifications. Thus, Film samples (10 mg cut into
313 small pieces) were mixed with 450 µl of distilled water. Then, 50 µl of 2 mM FeCl₂, 4 H₂O and
314 200 µl of 5 mM Ferrozine (3-(2-Pyridyl)-5,6-diphenyl-1,2,4-triazine) were added. The reaction
315 mixtures were vigorously stirred and incubated for 20 minutes at room temperature (25±2 °C).
316 The absorbance of the solutions was measured at 562 nm. Regarding the solutions of BTCP
317 powder, it was the same process used for all film samples. EDTA was used as positive control
318 and the inhibition percentage of ferrozine/Fe²⁺ complex formation was calculated using the
319 following equation:

$$320 \quad \text{Metal chelating activity (\%)} = \frac{[Abs_c + Abs_B - Abs_F]}{Abs_c} \times 100 \quad \text{Eq (10)}$$

321 where Abs_c is the absorbance of the control tube (without sample), Abs_B is the absorbance of
322 the blank tube and Abs_F is the absorbance of the sample in the presence of Ferrozine (reaction).

323 **2.7.10.3. Reducing power assay**

324 The ability to reduce iron (III) was determined using the Yildirim et al. (2001) method,
325 based on following up the ability of an antioxidant molecule to reduce ferric iron from
326 potassium ferricyanide (K₃Fe(CN)₆) in ferrous iron (Fe²⁺). Film samples (10 mg) and BTCP
327 solutions (1-4 mg) were immersed in 1.25 ml of 0.2 M phosphate buffer (pH 6.6) and 1.25 ml
328 of 1% (w/v) potassium ferricyanide, and incubated for 30 min at 50 °C. 1.25 ml of
329 trichloroacetic acid 10% (m/v) was added to the mixture in order to stop the reaction. Finally,
330 the mixture was centrifuged for 10 min at 3 500 g, and the supernatant (1.25 ml) was mixed
331 with 1.25 ml distilled water and 0.25 ml 1% (m/v) ferric chloride. After 10 min reaction, the
332 absorbance of the resulting solution was measured at 700 nm. Regarding the solutions of BTCP
333 powder, it was the same process used for all film samples. The values are presented as the
334 means of duplicate analyses. BHA was used as a standard for BTCP solutions.

335 **2.7.10.4. Total antioxidant activity (TAA)**

336 Total antioxidant activity was assayed using the method of Prieto et al. (1999). Briefly,
337 films were cut into small pieces (10 mg) and immersed in Eppendorf tubes containing 0.1 ml
338 of distilled water and 1 ml of reagent solution (0.6 M sulphuric acid, 28 mM sodium phosphate,
339 and 4 mM ammonium molybdate) and incubated at 90 °C for 90 min. Thereafter, the absorbance
340 was measured at 695 nm. Regarding the solutions of BTCP powder, it was the same process
341 used for all film samples. The total antioxidant activity of the films was expressed as α -
342 tocopherol equivalents using the following formula:

$$343 \quad C_{toc} (\mu\text{mol/mL}) = \frac{[OD_c/0.0049]}{0.011} \quad \text{Eq (11)}$$

344 where C_{toc} is the concentration as α -tocopherol equivalents ($\mu\text{mol/mL}$) and OD_s is the
345 absorbance of samples at 695 nm.

346 **2.8. Application of Cs-BTCP coating solutions**

347 *2.8.1. Preparation and coating treatments on shrimp*

348 Shrimps were purchased from a local fish store in Sfax, Tunisia. Only shrimps with a
349 uniform average weight, healthy appearance, good texture and no visible damage were selected
350 for the experimental work. First, shrimps were washed with running water and then dried in the
351 open air at room temperature. The shrimps were dipped into the respective coating solutions at
352 4 °C for 4-5 min. Then, the shrimps were placed in an air-tight sterile polyethylene boxes and
353 stored at 4 °C for 9 days. Shrimps were randomly divided into four groups (4 shrimps per group)
354 as follows: (**Sh**) control shrimp (uncoated) without treatment; (**Sh-1**) shrimp soaked in a coating
355 solution of Cs (2%, w/v); (**Sh-2**) shrimp dipped in a Cs90-10BTCP coating solution; (**Sh-3**)
356 shrimp coated with a Cs50-50BTCP coating solution. Finally, the samples from each group
357 were randomly taken out for analysis according to the predetermined time intervals (0, 3, 6 and
358 9 days of storage), in three replicates.

359 *2.8.2. Chemical evaluation*

360 pH of the shrimp was measured as described by Keller et al. (1974) by a pH-meter using
361 a mixture of 10 g of sample in 50 ml of distilled water.

362 The dry matter content was determined after evaporating the water contained in 5 g of
363 sample at 105 °C during 24 h until a constant weight was reached (Horwitz 2000).

364 Color was evaluated using a colorimeter Konica Minolta CR/5 (Sensing Europe B.V)
365 and expressed as L^* , a^* and b^* values, referring to the measuring parameters of lightness,
366 redness/greenness, and yellowness/blueness, respectively. Total color (ΔE) was determined as
367 mentioned above:

368
$$\Delta E = \frac{[a^* + 1.75 \times L^*]}{[5.645 \times L^* + a^* - 3.021 \times b^*]} \quad \text{Eq (12)}$$

369 *2.8.3. Determination of thiobarbituric acid reactive substances (TBARS)*

370 The thiobarbituric acid reactive substances (TBARS) test is widely used to evaluate lipid
371 peroxidation. The TBARS values were determined calorimetrically by the modified method of
372 Buege and Aust, (1972). Malondialdehyde (MDA) and other TBARS were evaluated based on
373 their reactivity with 2/thiobarbituric acid (TBA) under acidic conditions allowing a pink colored
374 complex detectable at 530 nm. In brief, a portion (0.5 g) of sample was homogenized with 625
375 μL of TBS (50 mM Tris containing 150 mM NaCl, pH 7.4) and 375 μl of TCA/BHT (TCA
376 20%, BHT 1%) in order to precipitate proteins, and then centrifuged (1000 g, 10 min, 4 °C).
377 Then, 400 μl of the supernatant were mixed with 80 μl of HCl (0.6 M) and 320 μl of Tris/TBA
378 (Tris 26 mM; TBA 120 mM). The homogenate was heated for 10 min at 90 °C. The absorbance
379 of the resulting solution was measured at 530 nm. TBARS values were expressed as milligram
380 of malonaldehyde equivalents per kilogram of sample.

381 *2.8.4. Determination of the conjugated dienes content*

382 Lipid oxidation was also assessed by the conjugated diene content using the method of
383 Srinivasan et al. (2011). The conjugated dienes were evaluated by increasing absorption at 233
384 nm.

385 *2.8.5. Determination of peroxide value*

386 The PV test was performed according to the method of Shantha and Decker, (1993) with
387 some modifications. The sample (0.30 g) was mixed with 9.8 ml chloroform–methanol in a
388 glass tube and vortexed for 2-4 s. Ammonium thiocyanate solution (10 mM) (0.05 ml) was
389 added and the sample was vortexed for 2-4 s. Then, 0.05 ml iron (II) solution was added and
390 the sample was vortexed for 2-4 s. Finally, the mixture was incubated for 5 min at room
391 temperature and the absorbance was determined at 500 nm. PV is expressed as milliequivalents
392 of peroxide oxygen combined in a kilogram of fat.

393 *2.8.6. Microbiological analysis*

394 Microbiological analysis of coated shrimps was determined by homogenizing 1 g of
395 shrimp sample in 9 ml of 0.9% NaCl at room temperature. Then, decimal dilutions were
396 prepared from the solution and plated in the appropriate media. The total psychrophilic aerobic
397 bacteria (TPAB) and the total mesophilic aerobic bacteria (TMAB) were estimated after
398 incubation for 48 h at 37 °C and for 7 days at 4 °C, respectively, using Plate Count Agar medium

399 (PCA). All microbial counts were converted to logarithms of colony/forming units per gram of
400 shrimp sample (log CFU/g).

401 2.9. Statistical analysis

402 All the measurements were realized in triplicate, based on the test used. All the statistical
403 computations were performed using SPSS ver. 20.0 professional edition (SPSS, Inc., Chicago,
404 IL, USA) via ANOVA analysis. All data were expressed as mean \pm standard deviation.
405 Differences were considered significant at $p < 0.05$.

406 3. Results and discussion

407 3.1. Characterization of bluefin tuna collagenous protein

408 3.1.1. Chemical analysis of BTCP

409 The collagenous proteins were successfully extracted from the head and cartilage of
410 bluefin tuna via a chemical and thermal treatments with an extraction yield of 8.10 g/100 g of
411 fresh by-products. The proximate composition, including protein, dry matter, moisture and ash
412 contents of BTCP, is presented in **Table 1**. BTCP showed high level of proteins (77.49%) and
413 low amount of fat (1.20%), revealing its high quality. The protein content of BTCP was higher
414 than that of snakehead fish protein concentrate (58.77%) (Romadhoni et al. 2016), but lower
415 than that of sardinella protein isolate (81.3%) (Azaza et al. 2022).

416 **Table 1:** Proximate composition of the bluefin tuna by-products and its collagenous protein
417 (BTCP)

	Bluefin tuna by- products	BTCP
Dry matter (%)*	36.94 \pm 0.87	93.04 \pm 0.85
Protein (%)**	72.84 \pm 0.31	77.49 \pm 0.35
Ash (%)**	17.37 \pm 0.48	20.76 \pm 0.42
Lipids (%)**	10.09 \pm 0.30	1.2 \pm 0.04
Yield (%)*	-	8.10

420 *: g dry matter per 100g wet matter, **: g dry matter per 100g dry matter. All the data are expressed
421 as mean \pm SD and are the mean of three replicates.

422 3.1.2. Antioxidant activities of BTCP

423 Since antioxidant compounds could act through several chemical mechanisms, the
424 antioxidant activity of BTCP was investigated through multiple assays, including the DPPH
425 radical scavenging, ferrous chelating activity, the reducing power and the total antioxidant
426 capacity (**Fig. 2**).

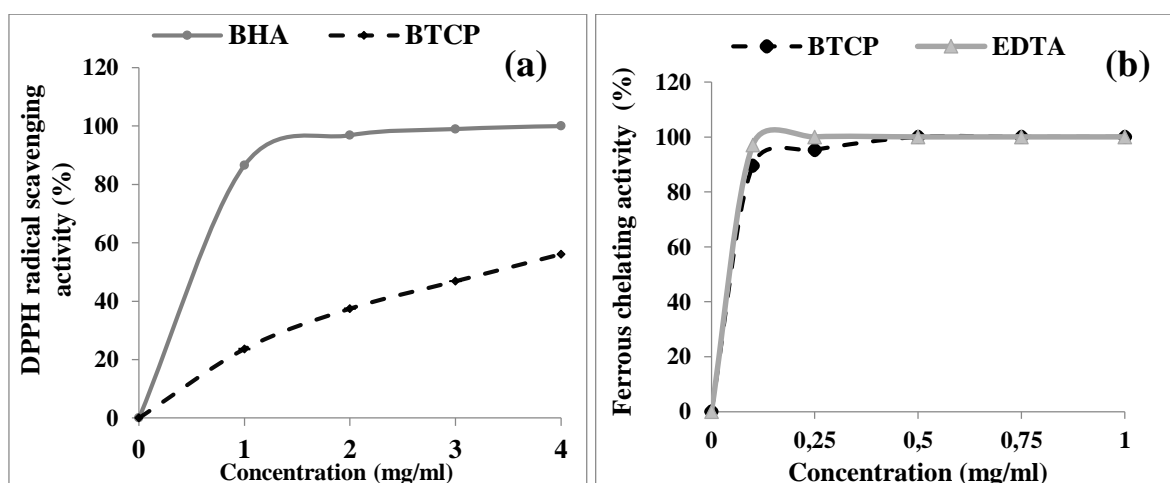
427 The DPPH radical scavenging activity of BTCP at various concentrations is shown in
428 **Fig. 2a**. The data revealed that the antioxidant activity of BTCP increased gradually with
429 increasing protein concentration. At a concentration of 4 mg/ml, the BTCP could scavenge
430 56.12% of the DPPH radicals (**Fig. 2a**). This could be attributed to the ability of BTCP to donate
431 hydrogen and stabilize the radical chain reaction leading to nontoxic species. The values of
432 antiradical scavenging activity of BTCP were significantly higher than that of rice bran protein
433 isolate which displayed 7.3% (Cho 2020).

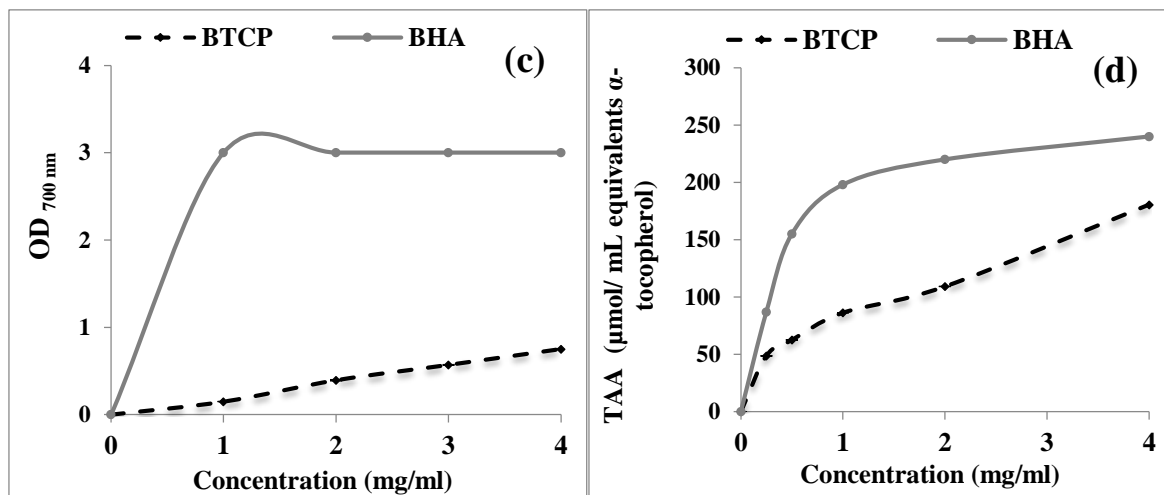
434 Furthermore, the ferrous chelating activity is illustrated in **Fig. 2b**. The BTCP showed a
435 chelating effect in a dose-dependent manner. In fact, BTCP displayed significant activity
436 reaching almost the same value as EDTA (100%) at the final concentration (1 mg/ml) (<0.05).
437 Therefore, BTCP could have the potential to improve the shelf life of food products and stop
438 efficiently their oxidative reaction.

439 However, for the reducing power assay, BTCP exhibited low reducing Fe^{3+} ions (**Fig. 2c**).
440 At 4 mg/ml, the reducing power of BTCP was 0.75 (OD_{700}), which was much lower than that
441 of BHA (control) at the same concentration ($\text{OD}_{700}=3$). It is worthy to note that, the BTCP
442 functions lightly as an electron donor. These results are slightly higher than those of rice bran
443 protein isolate reported by Cho (2020).

444 Lastly, **Fig. 2d** shows the calculated TAA expressed as α -tocopherol $\mu\text{mol/ml}$. The
445 obtained results revealed that the BTCP presented antioxidant activity, which increased
446 significantly with increasing protein concentrations ($P<0.05$) to reach 180 $\mu\text{mol/ml}$ at 4 mg/ml.
447 These findings suggest that increased values of TAA might have a protective ability against
448 oxidative stress induced by reactive oxygen species (ROS) (Alamdari et al. 2008).

449





450

451 **Fig. 2** DPPH radical scavenging activity (a), Chelating activity (b), Reducing power (c) and
 452 Total antioxidant activity (d) of BTCP

453 3.2. Characterization of Cs-BTCP composite films

454 3.2.1. Moisture content, water solubility and swelling degree of the Cs-BTCP composite films

455 The water-related characteristics of composite films, as well as MC, WS and SD results
 456 are presented in **Table 2**. The MC of films is critical for creating a favorable environment for
 457 food package films stability.

458 Regarding MC analysis, all tested films had similar moisture contents (about 20%). The
 459 obtained results are comparable to those of collagen-polysaccharide films reported by Ma et al.
 460 (2020). The reduction of MC value for composite films could be related to the interaction
 461 between chitosan and BTCP, which leads to a decrease in the water content in the film's network
 462 (Zhang et al. 2020). So, the low MC value of film permits protecting packaged food for a longer
 463 period. (Apriliyani et al. 2020).

464 The WS of composite films is shown in **Table 2**. Cs control film exhibited high water
 465 solubility of more than 57% (**Table 2**), which is slightly higher than WS values reported by
 466 Hamdi et al. (2019) and significantly lower than WS values stated by Kaya et al. (2018).
 467 Compared with the Cs100, the composite films had relatively lower WS values, reaching a
 468 value of 24% for Cs50-50BTCP ($p < 0.05$). Lower water solubility could be attributed to the
 469 hydrophobic properties of BTCP, which are involved in the weakness of the interactions
 470 between polymer-water.

471 Likewise, the swelling degree of the control chitosan film was 4.4 g/g as shown in **Table**
 472 **2**, which could be attributed to the hydrophilic property of chitosan (Moalla et al. 2021). As the
 473 content of BTCP increased, the SD of Cs-BTCP composite films tended to decrease ($p < 0.05$).

474 This decrease might be related to interactions between chitosan and BTCP, which leads
 475 the SD of the composite films to be lower than the control film. According to Di Pierro et al.
 476 (2006), the swelling degree of polymer films is closely correlated with the nature and the
 477 number of intermolecular chain interactions. These findings were similar to those stated by
 478 Zhang et al. (2020), with the addition of plant extracts, the SD of polysaccharide films
 479 decreased. Mathew et al. (2006) reported that the water diffusion and the breakdown of
 480 hydrogen and ionic bonds strongly depended on the solubility and swelling ability of films.

481 **Table 2:** Moisture content (MC), water solubility (WS), swelling degree (SD) and water vapor
 482 permeability (WVP) of Cs100 control film and Cs-BTCP composite films

Cs-BTCP ratios (v/v)	MC (%)	WS (%)	SD (g/g)	WVP ($\text{g}\cdot\text{s}^{-1}\cdot\text{m}^{-1}\cdot\text{Pa}^{-1}\times 10^{-10}$)
0/100	19 ± 0.84 ^a	57.68 ± 0.20 ^f	4.48 ± 0.01 ^f	4.26 ± 0.01 ^d
90/10	20.4 ± 0.28 ^a	50.30 ± 0.28 ^e	3.47 ± 0.04 ^e	4.12 ± 0.17 ^d
80/20	20.2 ± 0.41 ^a	47.38 ± 0.14 ^d	2.11 ± 0.01 ^d	4.02 ± 0.11 ^c
70/30	20.4 ± 1.03 ^a	43.00 ± 0.34 ^c	2.02 ± 0.11 ^c	3.40 ± 0.13 ^b
60/40	20.6 ± 1.13 ^a	33.21 ± 0.53 ^b	1.49 ± 0.01 ^b	3.33 ± 0.04 ^b
50/50	20.8 ± 1.31 ^a	24.06 ± 0.14 ^a	0.64 ± 0.04 ^a	3.10 ± 0.02 ^a

483
 484 **BTCP** : Bluefin tuna collagenous protein. **Cs**: Chitosan. Values are given as mean ± standard deviation (SD) of
 485 three independent tests. ^{a-f} different letters in the same column indicate a significant difference ($p < 0.05$). All
 486 films were previously stored at 25 °C and 50% RH.

487 The overall observations showed that the addition of BTCP decreased the hydrophilicity
 488 of the Cs-BTCP composite films, thus resulting in the decrease in the water solubility and
 489 swelling degree and in the improve in water resistance, implying their potential use as active
 490 food packaging materials that protect food, especially in humid environments (Pitak and
 491 Rakshit 2011).

492 3.2.2. Water vapor permeability

493 WVP is one of the most important physical properties to evaluate the reduction of water
 494 vapor transfer between the environment and food. The WVP should be as low as possible to
 495 preserve food quality and shelf life. The WVP of Cs-BTCP and Cs films was evaluated with a
 496 RH differential of 50% and the results are illustrated in **Table 2**. The Cs100 film showed the
 497 highest WVP value ($4.26 \times 10^{-10} \text{ g}\cdot\text{s}^{-1}\cdot\text{m}^{-1}\cdot\text{Pa}^{-1}$). The WVP of films significantly decreased by
 498 adding BTCP to the Cs film matrix, reaching a WVP value of $3.1 \times 10^{-10} \text{ g}\cdot\text{s}^{-1}\cdot\text{m}^{-1}\cdot\text{Pa}^{-1}$ for Cs50-
 499 50BTCP composite films. Numerous parameters may affect the WVP of film including the
 500 hydrophilic character of the polymer, the microstructure, and crosslinking degree in the

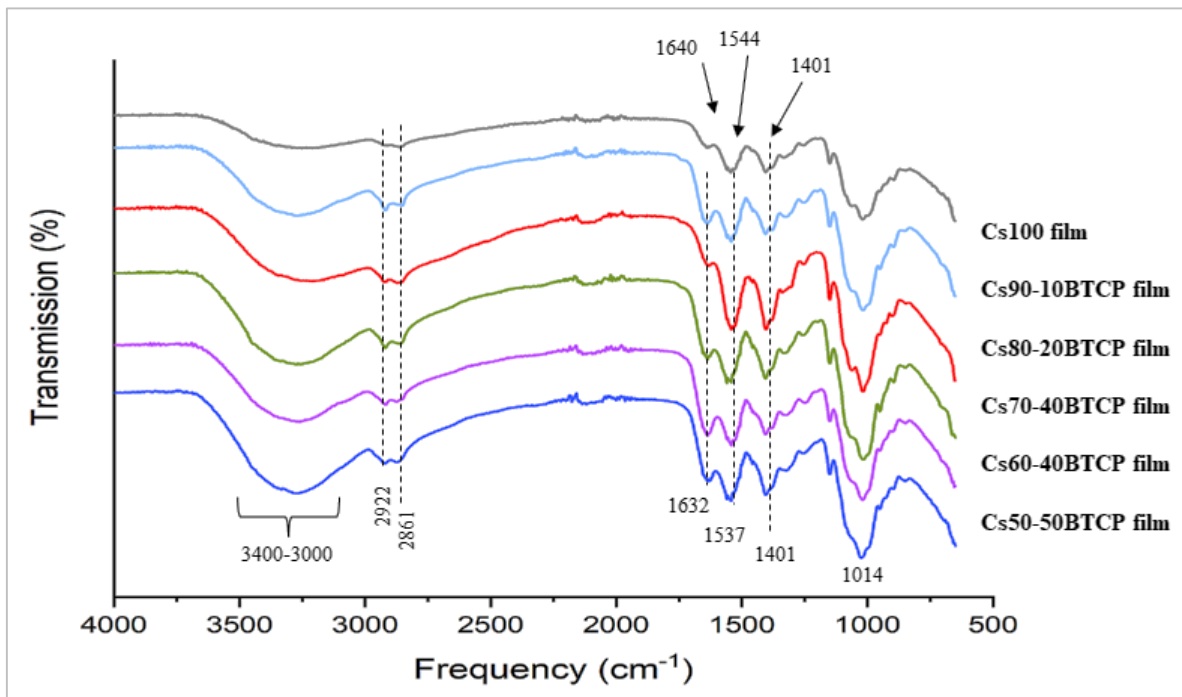
501 structure (Matta et al. 2019). The improvement of water barrier performance of composite films
502 could be attributed to the formation of intermolecular interactions between Cs and collagenous
503 proteins, leading to the increase of crosslinking degree and the decrease of the free volume of
504 the polymeric network and resulting, thereby, in the reduction of water transfer through the
505 composite film. The obtained result suggested that the addition of collagenous protein might
506 reduce the WVP of chitosan film based on its hydrophobic character, in accordance with
507 abovementioned results regarding WS and SD of Cs-BTCP films, inhibiting thereby the
508 diffusion of water vapor through the composite films. Similarly, (Zhang et al. 2019) found that
509 the WVP of the chitosan film was significantly ($p < 0.05$) reduced when the zein protein was
510 added and this was based on its hydrophobic character. Hence, Cs-based film incorporated with
511 BTCP had improved barrier water ability for potential application in food packaging.

512 3.2.3. FTIR spectroscopy analysis

513 FTIR spectroscopy is one of the most effective techniques for the identification of
514 molecular interactions in the composite films. The FTIR spectrum of Cs100 film shows a broad
515 absorption band at the range of $3400\text{--}3000\text{ cm}^{-1}$ assigned to the stretching vibrations of the O-
516 H and N-H groups (**Fig. 3**). The absorption bands detected at 2922 and 2861 cm^{-1} are
517 characteristic of symmetric and asymmetric C-H vibrations (Sun et al. 2017). Additionally,
518 specific bands for chitosan are detected, N-H (1544 cm^{-1}), -CH (1401 cm^{-1}), and glycosidic
519 cycles (1014 cm^{-1}) of chitosan. This trend is in line with previous work on changes in FT-IR
520 spectra occurring for chitosan-based composite film (Liu et al. 2018). As presented in **Fig. 3**,
521 all composite film peaks were roughly similar to those of Cs100 film showing major bands at
522 approximately $3400\text{--}3000$, $2922\text{--}2861$, 1632 , 1537 , 1401 and 1014 cm^{-1} , corresponding to
523 amides A (NH-stretching coupled with hydrogen bonding), amide B (asymmetric stretching
524 vibration of $=\text{C-H}$ and $-\text{NH}^{3+}$), amide-I (C=O stretching/hydrogen bonding coupled with $\text{C}=\text{C}$
525 C), amide-II (arising from bending vibration of N-H groups and stretching vibrations of C-N
526 groups), amide-III (vibrations in plane of C-N and N-H groups of bound amide or vibrations of
527 CH_2 groups) and glycosidic cycles, respectively.

528 When BTCP is added to the films, the wide peak at $3400\text{--}3000\text{ cm}^{-1}$ observed for Cs100
529 has changed to be more pronounced with the increase in BTCP concentration, indicating the
530 decreased stretching of the -NH and/or -OH available groups of chitosan contribute to the
531 hydrogen interactions between the BTCP-Cs bonds (Kaya et al. 2018). Moreover, there is a
532 shift in the region of amide-I (1640 cm^{-1}) and amide II (1544 cm^{-1}) to a lower wavenumber for
533 all composite films (1632 cm^{-1} and 1537 cm^{-1} , respectively). These outcomes indicate that the

534 formation of polysaccharide (Cs) and protein (BTCP) complexes is mainly due to the
535 interaction between the -COOH group on polysaccharide and groups -NH₃, -COOH on the
536 protein chain which are the sources of hydrogen bond between these two bio-polymers (Bealer
537 et al. 2020).



538

539 **Fig. 3** FTIR spectra of Cs100 film and Cs-BTCP composite films

539

540

541

542 3.2.4. X-ray diffraction analysis

543 The X-ray diffraction was conducted to investigate the changes in the morphology of
544 Cs-BTCP composite films. As shown in Fig. 4, Cs100 film diffractogram presents the
545 characteristic diffraction peaks at 2θ of 12° and 18°, attributed to high crystallinity of chitosan
546 (Li et al. 2013). Regarding composite films patterns, the intensity of the crystalline reflection
547 peaks decreased as the BTCP content increased compared to the Cs100 film. This finding could
548 be attributed to the destruction of crystalline structure of the Cs matrix and the formation of an
549 amorphous complex. Therefore, composite films had no strong diffraction peaks owing to
550 amorphous crystalline structures. Similar results were reported by Zhang et al. (2019), who
551 found that with the addition of zein to chitosan film formulation the intensity of peaks
552 decreased, reflecting the good compatibility between zein and chitosan chains.

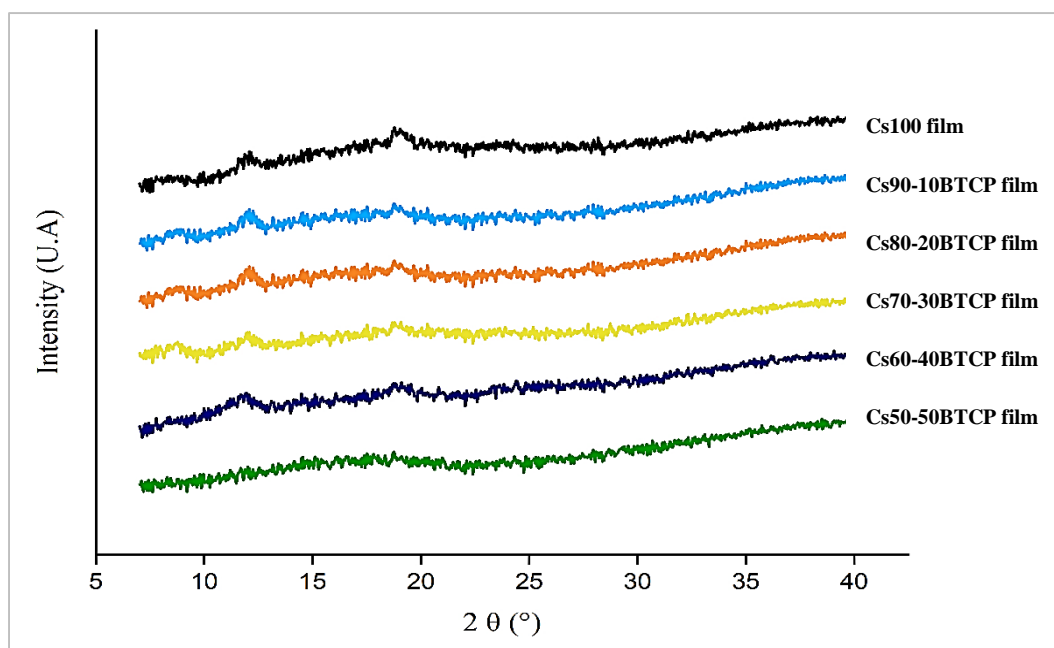


Fig. 4 XRD patterns of Cs100 film and Cs-BTCP composite films

553

554 3.2.5. Optical properties of composite films

555 The light-barrier property of packaging film is an important physical property, which
 556 protects the product against oxidation (Jiang et al. 2016). **Table 3** presents the transparency and
 557 the light transmittance of composite films in the wavelength range from 200 to 800 nm. Overall,
 558 the films incorporated with BTCP showed higher opacity values compared to the chitosan film.
 559 In addition, the UV-Vis absorption spectra show that the Cs100 film had poor light barrier
 560 property in the UV range, with a high transmission value of 23.7% at 280 nm. It is interesting
 561 to note that Cs-BTCP composite films have a low transmission of UV light at 280 nm, ranging
 562 from 0.01% to 6.59%. The decreased of UV-light penetration observed in our study is probably
 563 attributed to the presence of aromatic amino acids of proteins which absorb UV light below 380
 564 nm (Kalaycıoğlu et al. 2017).

565 As reported by Hajji et al. (2021), the incorporation of gelatin and shrimp protein
 566 hydrolysate improves the chitosan film's barrier property to the UV and visible light of chitosan
 567 film. Therefore, Cs-BTCP composite films could be used as UV-screening food packaging
 568 materials.

569 **Table 3:** Transmission of UV and visible lights and transparency of Cs100 film and Cs-BTCP
 570 composite films

Cs-BTPC ratios (v/v)	Light transmittance in different wavelengths (nm)								Transparence
	200	280	350	400	500	600	700	800	

0/100	0.1	23.7	50	65.01	80.72	85.9	86.29	86.29	0.143±0.02 ^b
90/10	0.1	6.59	18.87	31.91	45.81	53.57	57.67	60.67	0.047±0.00 ^a
80/20	0.1	0.65	4.37	14.62	31.11	39.15	43.85	46.66	0.045±0.04 ^a
70/30	0.1	0.39	4.46	11.27	23.06	30.76	36.22	40.83	0.041±0.01 ^a
60/40	0.1	0.99	4.84	8.91	15.84	22.43	27.86	32.88	0.032±0.01 ^a
50/50	0.1	0.1	1.1	4.32	13.3	19.72	24.83	29.24	0.026±0.01 ^a

571 **BTCP** : Bluefin tuna collagenous protein ; **Cs**: Chitosan. ^{a-b} different letters in the same column indicate a
572 significant difference (p < 0.05).
573

574 The color of the film is an interesting optical property that influences the appearance and
575 the marketing value of the packaging. As seen in **Table 4**, there was no significant L* values
576 (lightness) difference among all films (p > 0.05). All the films had low L* values that did not
577 exceed L*=32. This property may contribute to preventing oxidative degradation of packaged
578 foods due to exposure to visible and ultraviolet light, which causes nutrient loss, off-flavors,
579 and discoloration. However, the color of composite films changed to a more yellow color with
580 increasing BTCP concentrations (**Table 4**). Similar results has been reported by our previous
581 study (Azaza et al. 2022), when adding sardinella protein isolate to chitosan film matrix.

582

583

584

585 **Table 4:** Color parameters (L*. a*. b*) and total color difference (ΔE*) for Cs100 control film
586 and Cs-BTCP composite films

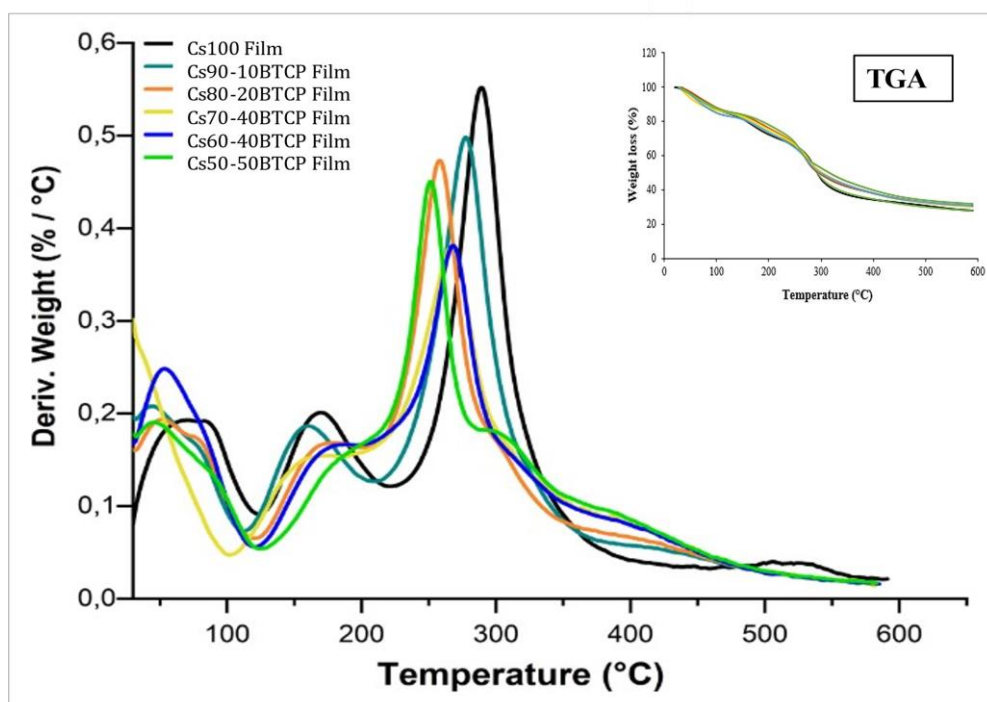
Cs-BTCP ratios (v/v)	L*	a*	b*	ΔE
0/100	29.35±0.18 ^a	-0.1±0.01 ^f	0.285±0.03 ^a	—
90/10	30.51±0.09 ^b	-0.52±0.00 ^d	0.61±0.00 ^b	1.79±0.08 ^a
80/20	31.52±0.77 ^c	-0.50±0.00 ^c	0.60±0.01 ^c	2.55±0.58 ^b
70/30	31.97±0.28 ^c	-0.42±0.06 ^e	1.11±0.07 ^d	2.72±0.11 ^b
60/40	32.04±0.70 ^c	-0.63±0.15 ^{ab}	1.29±0.02 ^e	3.38±0.50 ^c
50/50	31.99±0.72 ^c	-0.75±0.04 ^a	1.71±0.08 ^f	3.62±0.50 ^c

587 **BTCP** : Bluefin tuna collagenous protein ; **Cs** : Chitosan. Values are given as mean ± standard deviation
588 (SD) of three independent tests. ^{a-f} different letters in the same column indicate a significant difference (p <
589 0.05).

590 *3.2.6. Thermogravimetric analysis (TGA)*

591 The effect of BTCP addition on the thermal stability of composite films was investigated.
592 The obtained TGA thermograms of films and their derivative (DTG) are shown in **Fig. 5**. The
593 weight loss curve of the Cs100 film presents three distinct phases. The first one (peak I)
594 occurred between 50 and 125 °C, corresponding to the evaporation of water and residual solvent
595 in the film (Altiok et al. 2010). The second weight loss (peak II) detected at 168 °C may be
596 ascribed to degradation of glycerol (Kaya et al. 2018; Kamdem et al. 2019). Finally, the third
597 stage of weight loss (peak III), related to the pyrolytic decomposition of the chitosan matrix, is
598 recorded at 288 °C (de Britto and Campana-Filho 2007).

599 Notably, for a small amount of BTCP (10%; w/w polymer), a slight shift towards 278 °C
600 was observed, indicating a maintenance of thermal stability similar to chitosan film.
601 Nevertheless, at higher amounts of BTCP (20%, 30%, 40% and 50%; w/w polymer), the weight
602 loss of the decomposition of the chitosan matrix in Cs-BTCP films shifted to lower values,
603 reaching 267 °C, 267 °C, 257 °C and 251 °C, respectively (**Fig. 5**), resulting in reduced thermal
604 stability of composite films. The reduction of the thermal stability could be related to the
605 decrease of the crystallinity of the composite films as reported by the XRD assay. These results
606 are consistent with those reported by Song et al. (2020), which shows that the incorporation of
607 magnolol into the chitosan film results in an decrease in the thermal degradation temperature,
608 thus a low thermal stability of the magnolol-chitosan film.



609
610 **Fig. 5** TGA and DTG thermograms of Cs100 control film and Cs-BTCP composite films

611 *3.2.7. Mechanical properties*

612 The thickness of composite films was measured, and results reveal that Cs-BTCP
 613 composite films exhibited higher thicknesses than Cs100 film (**Table 5**). The thicknesses of
 614 composite films gradually increased with the increase of BTCP content from 31 μm for Cs90-
 615 10BTCP to 52 μm for Cs50-50BTCP ($p < 0.05$). Arancibia et al. (2015) also found that the
 616 incorporation of protein concentrate increased the film thickness. The increase of composite
 617 film thickness can be attributed to the increase of BTCP content on the Cs film matrix, leading
 618 to the increase of solids content, and thus a change in the compaction of chitosan, glycerol, and
 619 BTCP molecules (Costa et al. 2018; Na et al. 2018).

620 Tensile strength and elongation at break were usually related to the film network
 621 microstructure and the intermolecular force. The TS and EAB values of Cs and Cs-BTCP films
 622 were measured and reported in **Table 5**. Results revealed that the Cs100 film showed the highest
 623 TS and EAB values of 20.23 MPa and 12.64%, respectively. For Cs10-90BTCP, no significant
 624 change was noted for the TS (19.51 MPa) and EAB (11.27%) values ($p > 0.05$), suggesting good
 625 compatibility and effective crosslinking between BTCP and chitosan. However, at higher BTCP
 626 concentration, the TS and EAB values decreased significantly ($p < 0.05$). These findings
 627 revealed that the Cs-BTCP films were less resistant and elastic, giving therefore a less
 628 deformable film structure, compared to control film. Thus, the higher content of BTCP leads to
 629 the formation of agglomerated particles in the composite film, destroying, thereby, the compact
 630 structure of Cs films and reducing the molecular mobility and flexibility of the chitosan matrix
 631 (Hajji et al. 2021; Azaza et al. 2022).

632
 633 **Table 5:** Tensile strength (TS. %), elongation at the break (EAB. MPa) and thickness (μm) of
 634 Cs100 control film and Cs-BTCP composite films
 635

Cs-BTCP ratios (v/v)	EAB (%)	TS (MPa)	Thickness (μm)
0/100	12.64 ± 0.26^d	20.23 ± 0.18^e	13.5 ± 0.02^a
90/10	11.27 ± 0.49^c	19.51 ± 0.09^d	31.5 ± 0.0^b
80/20	9.51 ± 0.18^b	18.92 ± 0.23^c	34 ± 0.00^c
70/30	8.93 ± 0.32^a	19.09 ± 0.38^c	38.5 ± 0.04^d
60/40	8.70 ± 0.38^a	13.67 ± 0.84^b	46.5 ± 0.01^e
50/50	8.72 ± 0.39^a	4.87 ± 0.06^a	52.5 ± 0.0^f

636 **BTCP** : Bluefin tuna collagenous protein; **Cs**: Chitosan. Values are given as mean \pm standard deviation (SD) of
 637 three independent tests. ^{a-f} different letters in the same column indicate a significant difference ($p < 0.05$).

638 *3.2.8. Antioxidant potential of Cs and BTCP composite films*

639 The effect of incorporating BTCP at different contents on antioxidant activity of chitosan
 640 films was studied. The results, illustrated in **Table 6**, show that increasing BTCP content
 641 improve the chelating effect of composite films (98.59-99.5%) compared to the Cs100 film
 642 (36%). Similarly, the DPPH scavenging activity of composite films (90.17-94.08%) was
 643 significant higher that the Cs100 film (74.1%) as the BTCP increase.

644 As shown in **Table 6**, a higher reducing power was correlated with the addition of BTCP
 645 into chitosan matrix, reaching a value of $OD_{700}=1.24$. The control film presented the lowest
 646 ability to reduce ferric ion ($OD_{700}=0.165$) (Hamdi et al. 2019). This capacity was significantly
 647 enhanced for Cs-BTCP composite films.

648 Lastly, total antioxidant results of composite films are reported in **Table 6**. The control
 649 film has a low antioxidant activity ($12.51 \mu\text{mol/mL}$ equivalents α -tocopherol). However, films
 650 supplemented with BTCP exhibited a relatively high antioxidant activity, which increased
 651 significantly with increasing BTCP content reaching approximately $40.33 \mu\text{mol/mL}$
 652 equivalents α /tocopherol for Cs50-50BTCP. It is worthy to note that BTCP could convert Mo
 653 (VI) to Mo (V) which is more stable.

654 The significantly high total antioxidant capacity of the composite films could be attributed
 655 to the incorporation of BTCP, which showed a distinct antioxidant potential in a dose-dependent
 656 manner evaluated in this study by different in vitro antioxidant assays. In addition, it may also
 657 be related to the interaction or hydrogen bonds between the functional groups of the added
 658 BTCP and those of the chitosan matrix (Kchaou et al. 2017).

659 **Table 6:** Antioxidant activities of Cs100 control film and Cs-BTCP composite films

Cs-BTCP ratios (v/v)	Metal chelating effect (%)	Reducing power (OD_{700})	DPPH radical scavenging activity (%)	Total antioxidant capacity ($\mu\text{mol/ mL}$ équivalents α -tocophérol)
0/100	36.00 ± 0.02^a	0.165 ± 0.009^a	74.1 ± 0.58^a	12.51 ± 0.71^a
90/10	98.59 ± 0.28^d	0.53 ± 0.02^b	90.17 ± 0.22^b	13.10 ± 0.13^a
80/20	96.03 ± 0.22^b	0.67 ± 0.005^c	90.97 ± 0.07^b	21.37 ± 0.51^b
70/30	96.32 ± 0.37^b	0.77 ± 0.00^d	91.26 ± 0.44^c	32.92 ± 0.44^c
60/40	97.52 ± 0.12^c	0.98 ± 0.03^e	92.44 ± 0.36^c	35.60 ± 0.96^d
50/50	99.50 ± 1.57^e	1.24 ± 0.08^f	94.08 ± 0.80^c	40.33 ± 0.71^e

660 **BTCP** : Bluefin tuna collagenous protein; **Cs** : Chitosan. Values are given as mean \pm standard deviation (SD) of
 661 three independent tests. ^{a-f} different letters in the same column indicate a significant difference ($p < 0.05$).
 662

663 3.3. Coating of shrimp

664 *3.3.1. Chemical analysis*

665 The bio-based coatings present a useful and economical technique for shrimp covering,
 666 which might preserve and extend food shelf life (Costa et al. 2018b). In this context, the Cs100
 667 bioactive film, used as a control coating, as well as the Cs90-10BTCP and Cs50-50BTCP films,
 668 were applied for the preservation of shrimp quality. These different coatings were advantageous
 669 with respect to functionality, good stability, mechanical behavior and noticeable antioxidant
 670 capacity. To assess the preservative effect of these coatings, moisture content and pH value of
 671 coated shrimp samples were measured after 9 days of storage at 4°C and compared to those of
 672 uncoated shrimp (**Table 7**).

673 The moisture of the uncoated pieces of shrimp was assigned a value of 23.23% after 9
 674 days of storage. However, coating with chitosan film/forming solution contributed to the
 675 increase in moisture, showing values of 24.27%. The addition of BTCP significantly increased
 676 the moisture content of coated shrimp, which was approximately 25.58% and 25.63%, for
 677 coated shrimp Sh-2 and Sh-3, respectively.

678 In addition, the effect of Cs-BTCP coating solution on the pH change of shrimp after 9
 679 days of refrigerated storage is presented in **Table 7**. The results revealed that there were no
 680 changes in pH values occurred for shrimp samples after 9 days. The mixture of Cs and BTCP
 681 had a significant impact on the shrimp freshness compared to Cs alone. These results are in
 682 accordance with those reported by Xiong et al. (2020), suggesting that the incorporation of GSE
 683 and/or nisin did not affect the pH value of the coated meat during storage.

684 Previous studies have shown that there are three levels of quality based on the pH value,
 685 as follows: prime quality (<7.7), poor but acceptable quality (7.70-7.95) and unacceptable
 686 quality (> 7.95) (Marshall and Wiese-Lehigh 1997). In our study, it was shown that the pH was
 687 placed in the first level, suggesting that the coatings of Cs and Cs-BTCP mixtures were effective
 688 in preserving the quality of shrimp compared to uncoated shrimp.

689 **Table 7:** Changes in MC, pH, color parameters and microbial parameters (TPF: total
 690 psychrotrophic flora. TMF: total mesophilic flora) of shrimp samples at 0 and 9 days of storage
 691

Parameters	Days	Sh	Sh-1	Sh-2	Sh-3
MC	0	21.22±0.01 ^{aA}	22.90±0.02 ^{aC}	27.53±0.02 ^{bD}	22.17±0.07 ^{aB}
	9	23.23±0.07 ^{aB}	24.27±0.04 ^{bB}	25.85±0.01 ^{aD}	25.63±0.12 ^{bC}
pH	0	7.86±0.01 ^{bB}	7.22±0.01 ^{bA}	7.22±0.07 ^{aA}	7.25±0.01 ^{bA}
	9	7.76±0.01 ^{aB}	7.18 ±0.02 ^{aA}	7.20±0.07 ^{aA}	7.22±0.01 ^{aA}

L*	0	55.67±0.13 ^{bA}	57.85±0.03 ^{bC}	57.64±0.13 ^{bB}	58.74±0.10 ^{bD}
	9	54.73±0.06 ^{aA}	56.05±0.31 ^{aB}	56.27±0.33 ^{aC}	56.15±0.62 ^{aBC}
a*	0	2.78±0.01 ^{aD}	2.57±0.01 ^{aC}	2.35±0.06 ^{aB}	2.18±0.03 ^{bA}
	9	4.71±0.13 ^{bD}	3.56±0.04 ^{bC}	2.71±0.40 ^{aB}	2.31±0.07 ^{aA}
b*	0	5.07±0.09 ^{aA}	5.15±0.11 ^{aA}	7.55±0.23 ^{aB}	7.98±0.42 ^{aB}
	9	5.20±0.01 ^{bA}	8.46±0.04 ^{bB}	8.84±0.06 ^{bB}	12.01±0.28 ^{bC}
ΔE	0	-	2.20±0.11 ^{aB}	3.20±0.15 ^{aC}	4.28±0.33 ^{aD}
	9	-	3.70±0.27 ^{bB}	4.43±0.39 ^{bB}	8.23±0.63 ^{bC}
Browning Index (%)	0	12.22±0.19 ^{aA}	12.83±0.20 ^{aA}	16.57±0.56 ^{aB}	16.86±0.37 ^{aB}
	9	15.83±0.17 ^{bA}	20.08±0.78 ^{bB}	20.50±0.01 ^{bB}	23.72±0.50 ^{bC}
TPAB (log UFC/g)	0	0.38±0.04 ^{aA}	-	-	-
	9	1.97±0.02 ^{bD}	1.10±0.02 ^c	0.39±0.04 ^b	0.34±0.02 ^a
TMAB (log UFC/g)	0	0.21±0.02 ^{aA}	-	-	-
	9	4.67±0.04 ^{bD}	1.13±0.03 ^c	0.60±0.01 ^b	0.46±0.02 ^a

692 **Sh** : control shrimp (uncoated) with no treatment; **Sh-1** : shrimp dipped in Cs solution; **Sh-2** : shrimp dipped in
693 Cs90-10BTCP solution; **Sh-3** : shrimp coated with Cs50/50BTCP solution. ^(a-d) Different letters indicate significant
694 differences between different samples on the same storage day ($p < 0.05$). ^(A-D) Different letters in each column
695 mean a significant difference for the same sample on different storage days ($p < 0.05$).

696 Color is a key factor for consumers to determine the quality of the seafood product.
697 Therefore, the quality of shrimps can be correlated with the skin color browning and/or
698 darkening which results from biochemical reactions with the ripening process during prolonged
699 storage. The changes in color indices (L^* , a^* , b^* , ΔE and BI) of control and coated shrimps
700 during storage at 4 ± 1 °C can be expressed by color indices (**Table 7**). The color of the uncoated
701 shrimp changed after 9 days of storage. The lightness (L^*) value of uncoated shrimp decreased,
702 and the redness (a^*) value increased. The values were higher than those of coated ones. Chitosan
703 coatings (Sh-1) had a positive effect on the L^* , a^* and b^* values. They increased for chitosan
704 coated shrimps while they decreased for the uncoated one. Therefore, the coating of shrimp by
705 Cs-BTCP coating solutions lead to stability of its lightness (L^*), a significant increase of its
706 yellowness (b^*) and a clear decrease in the values of the redness (a^*). However, it is important
707 to note that the BTCP incorporation positively resulted in lower redness and higher yellowness
708 values due to its initial yellow color. In addition, there was a gradual increase in browning index
709 values (%) suggests a progressively higher rate of enzymatic browning (Kortei et al. 2015).
710 Thus, the Cs-BTPC composite films showed a reduction in color indices of shrimp during
711 storage.

712 Generally, there was a gradual increase in the ΔE values of shrimp for the three groups
713 with the storage time increasing. This was especially apparent in the Sh-3 which has
714 significantly higher ΔE values than the other groups (**Table 7**).

715 3.3.2. Peroxide value

716 The most commonly used measure to evaluate autoxidation quality is the peroxide value
717 (PV), which determines the primary lipid oxidation products. The PV values were measured to
718 assess the effectiveness of the Cs-BTCP coating solution in preventing the auto-oxidation of
719 lipids in shrimp (Gray et al. 1996). From the second day until the end of the storage period, PV
720 levels of uncoated shrimp gradually increased ($p < 0.05$). For untreated shrimp, the PV value
721 increased from 0.015 meq O₂/kg to 0.03 meq O₂/kg of fat on the ninth day of storage (**Fig. 6a**).
722 However, the PV values of coated shrimp were considerably lower ($p < 0.05$) than the uncoated
723 shrimp. On the ninth day of storage, the chitosan coating slightly delayed peroxidation of fat
724 reaching a value of 0.022 meq O₂/kg fat. It is interesting to note that the PV values of Sh-2 and
725 Sh-3 coating solutions were 0.019 and 0.017 meq peroxides/kg lipid after 9 days of storage,
726 respectively. Thus, the addition of BTCP improves the antioxidant activity of chitosan coating
727 solution, leading, thereby, to the reduction shrimp peroxidation.

728 Similarly, in a previous study (Azaza et al. 2022), we affirmed that chitosan-sardinella
729 protein isolate packaging films might reduce the production of primary lipid oxidation products
730 in the shrimp under refrigerated storage.

731 3.3.3. Conjugated dienes (CD)

732 Lipid oxidation was estimated by the measurement of conjugated dienes (CD) content.
733 The results, presented in **Fig. 6b**, show the increase in CD values over the shelf/life for all
734 samples. In fact, the highest value of CD was noted in uncoated shrimp (Sh) and shrimp coated
735 with a film/forming solution of Cs100 (Sh-1) reaching an OD of 0.47 and 0.31 at day 9,
736 respectively. It is worthy to note that Sh-2 and Sh-3 showed the lowest OD values of 0.27 and
737 0.24 ($p < 0.05$), respectively, demonstrating that the addition of the BTCP in the Cs film/forming
738 solution was effective in CD development delay. Therefore, BTCP could be considered as
739 interesting antioxidant additive that can prevent the oxidation of food.

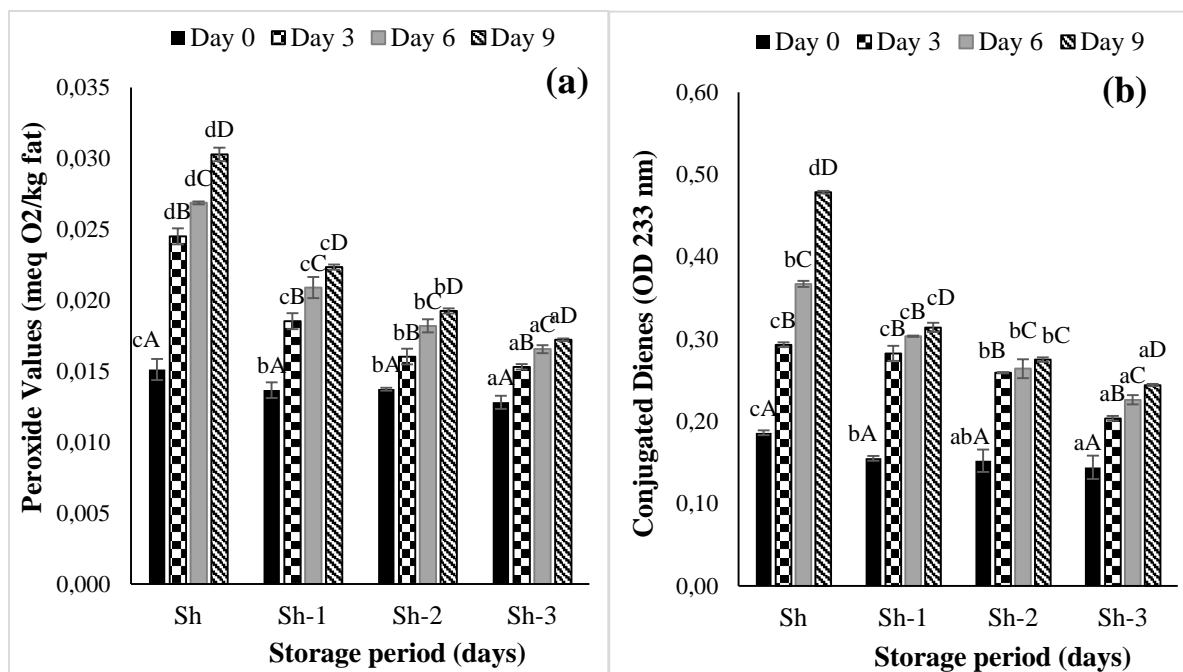
740 3.3.4. TBARS test

741 The lipid oxidation of the shrimp sample was also investigated through the measures of
742 the content malondialdehyde (MDA). MDA is defined as a biomarker of oxidative damage to
743 lipids. As shown in **Fig. 6c**, an increase in MDA content was observed for uncoated shrimp

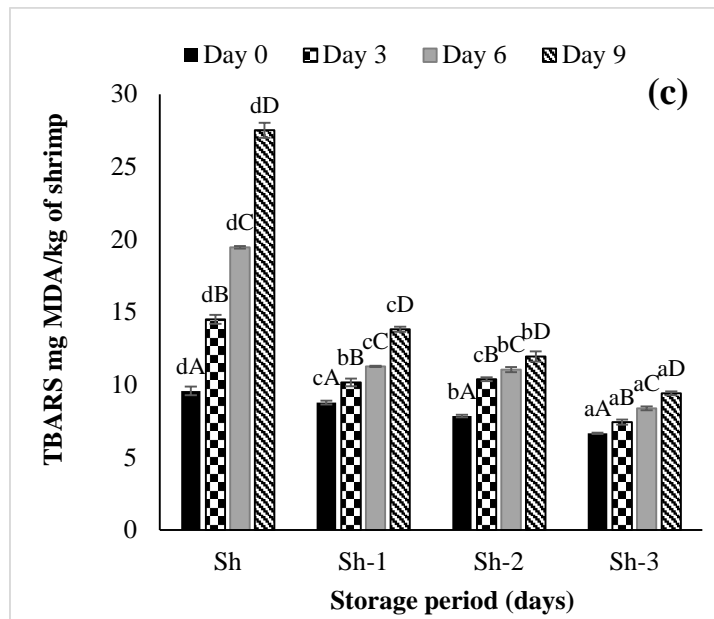
744 (Sh) samples after 9 days of storage at 4°C. In fact, TBARS value increased from 9.57 mg
 745 MDA/kg on day 0 to 27.51 mg MDA/kg on day 9 (**Fig. 6c**).

746 As compared to the uncoated shrimp (Sh), the extent of secondary oxidation is
 747 significantly lower ($p < 0.05$) in the samples coated by Cs film solution enriched with BTCP,
 748 reaching 13.81; 11.94 and 9.41 mg MDA/kg on day 9 for (Sh-1), (Sh-2) and (Sh-3),
 749 respectively. Hence, the combination of chitosan and BTCP resulted in the reduction of MDA
 750 formation.

751 It is worth mentioning that both antioxidant and oxygen barrier properties of chitosan
 752 coating may have contributed to the control of lipid oxidation in the shrimp but also the
 753 incorporation of BTCP in Cs coating with different concentrations, had an inhibitory role
 754 against lipid peroxidation. Farajzadeh et al. (2016) found that the TBARS values of shrimp
 755 samples with chitosan/gelatin coatings had much slower increase during frozen storage.



756



757
 758 **Fig. 6** Effect of BTCP incorporation (10% and 50%, w/w polymer) in the chitosan film matrix
 759 on peroxide value (meq O₂/kg fat) (a), conjugated dienes (OD 233 nm) (b) and thiobarbituric-
 760 acid reactive substances values (mg MDA/kg) (c) of coated shrimps during refrigerated period.

761 (a-d) Different letters indicate significant differences between different samples on the same storage day (p < 0.05).
 762 (A-D) Different letters in each column mean a significant difference for the same sample on different storage days
 763 (p < 0.05)

764 *3.3.5. Microbial analysis*

765 Effects of coatings on the microbiological quality of shrimp stored at 4 °C are shown in
 766 **Table 7**. The initial total psychrophilic aerobic bacteria (TPAB) and total mesophilic aerobic
 767 bacteria (TMAB) counts for control shrimp were approximately 0.38 and 0.21 (log CFU/g),
 768 respectively, signifying a high initial quality of the shrimp. Over the 9 days storage period, the
 769 TPAB and TMAB of the control shrimp samples increased quickly to 1.97 and 4.67 log CFU/g,
 770 respectively (p<0.05). However, coating shrimp with chitosan film/forming solution reduced
 771 the growth of micro/organisms, reaching values of about 1.10 and 1.13 log CFU/g for TPAB
 772 and TMAB, respectively. Furthermore, Cs50-50 BTCP and Cs90-10BTCP film forming
 773 solution were able to reduce significantly the TPAB and TMAB counts, comparing to the Cs100
 774 one. Hence, the incorporation of BTCP to chitosan film forming solution demonstrated an
 775 excellent barrier effect around shrimp against bacterial proliferation and oxygen diffusion.
 776 Additionally, it is notable that the Cs-BTCP ratio of 90:10 is enough to reduce 2.8/fold and
 777 1.8/fold, respectively, the growth of TPAB and TMAB, in comparison to the Cs100 solution.
 778 These findings are in accordance with those reported by Mohebi and Shahbazi, (2017), who
 779 confirmed that chitosan and gelatin coatings can be used as an active packaging to delay the
 780 growth of spoilage microorganisms and extend the shelf life of the shrimp of at least 11 days.

781 **Conclusion**

782 Composite films based on Cs and BTCP were successfully developed. The properties
783 of the resulted films are dependent on the Cs-BTCP ratio. FTIR analysis are very effective in
784 identifying polymer compositions and their compatibility. The resulting Cs-BTCP composite
785 films showed improved antioxidant activity, reduced WS, SD, light transmittance and WVP
786 properties, as compared to the Cs100 film. Interestingly, the composite films prepared at a Cs-
787 BTCP ratio of 90:10 (v/v) showed interesting mechanical and thermal stability similar to the
788 Cs100 film. The obtained results indicated the incorporation of BTCP improved the chitosan
789 film functionality. Additionally, the Cs-BTCP coating solution was effective in preserving the
790 good quality of shrimp, as it prevented the bacteria growth and decreased the oxidation of
791 coated shrimp.

792 **CRedit authorship contribution statement**

793 **Youssra Ben Azaza:** Conceptualization, Methodology, Investigation, Validation,
794 Formal analysis, Visualization, Writing – original draft; **Marwa Hamdi:** Investigation and
795 Methodology; **Christophe Charmette:** Investigation and Methodology; **Arie Van der lee:**
796 Investigation and Methodology; **Mourad jridi:** Investigation; **Suming Li:** Funding acquisition,
797 Supervision; **Moncef Nasri:** Supervision, Editing and Validation; **Rim Nasri:** Resources,
798 Supervision, Funding acquisition, Writing - review & editing.

799 **Declaration of competing interest**

800 All cited authors certify that they have sufficiently participated in the work to assume
801 public responsibility for the content. The authors declare that there is no conflict of interest
802 regarding the publication of this article.

803 **Acknowledgements**

804 This research work was funded by the Ministry of Higher Education and Scientific
805 Research, Tunisia and financed by the joint French-Tunisian PHC Utique Program (grant N°:
806 19G0815).

807 **References**

808 Affes S, Aranaz I, Hamdi M, et al (2019) Preparation of a crude chitosanase from blue crab
809 viscera as well as its application in the production of biologically active chito-
810 oligosaccharides from shrimp shells chitosan. *International Journal of Biological*
811 *Macromolecules* 139:558–569. <https://doi.org/10.1016/j.ijbiomac.2019.07.116>

- 812 Aider M (2010) Chitosan application for active bio-based films production and potential in the
813 food industry: Review. *LWT - Food Science and Technology* 43:837–842.
814 <https://doi.org/10.1016/j.lwt.2010.01.021>
- 815 Al Khawli F, Pateiro M, Domínguez R, et al (2019) Innovative green technologies of
816 intensification for valorization of seafood and their by-products. *Marine Drugs* 17:689.
817 <https://doi.org/10.3390/md17120689>
- 818 Alamdari DH, Ghayour-Mobarhan M, Tavallaie S, et al (2008) Prooxidant-antioxidant balance
819 as a new risk factor in patients with angiographically defined coronary artery disease.
820 *Clin Biochem* 41:375–380. <https://doi.org/10.1016/j.clinbiochem.2007.12.008>
- 821 Altioek D, Altioek E, Tihminlioglu F (2010) Physical, antibacterial and antioxidant properties of
822 chitosan films incorporated with thyme oil for potential wound healing applications. *J*
823 *Mater Sci Mater Med* 21:2227–2236. <https://doi.org/10.1007/s10856-010-4065-x>
- 824 Aranaz I, Alcántara AR, Civera MC, et al (2021) Chitosan: An overview of its properties and
825 applications. *polymers (Basel)* 13:3256. <https://doi.org/10.3390/polym13193256>
- 826 Arancibia MY, Alemán A, López-Caballero ME, et al (2015) Development of active films of
827 chitosan isolated by mild extraction with added protein concentrate from shrimp waste.
828 *Food Hydrocolloids* 43:91–99. <https://doi.org/10.1016/j.foodhyd.2014.05.006>
- 829 Azaza YB, Hamdi M, Charmette C, et al (2022) Development and characterization of active
830 packaging films based on chitosan and sardinella protein isolate: Effects on the quality
831 and the shelf life of shrimps. *Food Packaging and Shelf Life* 31:100796.
832 <https://doi.org/10.1016/j.fpsl.2021.100796>
- 833 Barlow CY, Morgan DC (2013) Polymer film packaging for food: An environmental
834 assessment. *Resources, Conservation and Recycling* 78:74–80.
835 <https://doi.org/10.1016/j.resconrec.2013.07.003>
- 836 Bealer EJ, Onissema-Karimu S, Rivera-Galletti A, et al (2020) Protein–polysaccharide
837 composite materials: fabrication and applications. *Polymers* 12:464.
838 <https://doi.org/10.3390/polym12020464>
- 839 Bersuder P, Hole M, Smith G (1998) Antioxidants from a heated histidine-glucose model
840 system. I: Investigation of the antioxidant role of histidine and isolation of antioxidants
841 by high-performance liquid chromatography. *J Amer Oil Chem Soc* 75:181–187.
842 <https://doi.org/10.1007/s11746-998-0030-y>
- 843 Buege JA, Aust SD (1972) On the solubilization of NADPH-cytochrome c reductase from rat
844 liver microsomes with crude pancreatic lipase. *Biochimica et Biophysica Acta (BBA) -*
845 *General Subjects* 286:433–436. [https://doi.org/10.1016/0304-4165\(72\)90284-X](https://doi.org/10.1016/0304-4165(72)90284-X)
- 846 Caruso G, Floris R, Serangeli C, Di Paola L (2020) Fishery wastes as a yet undiscovered
847 treasure from the sea: biomolecules sources, extraction methods and valorization.
848 *Marine Drugs* 18:622. <https://doi.org/10.3390/md18120622>
- 849 Cho S-J (2020) Changes in the antioxidant properties of rice bran protein isolate upon simulated
850 gastrointestinal digestion. *LWT* 126:109206. <https://doi.org/10.1016/j.lwt.2020.109206>

- 851 Costa MJ, Maciel LC, Teixeira JA, et al (2018a) Use of edible films and coatings in cheese
852 preservation: Opportunities and challenges. *Food Research International* 107:84–92.
853 <https://doi.org/10.1016/j.foodres.2018.02.013>
- 854 Costa MJ, Maciel LC, Teixeira JA, et al (2018b) Use of edible films and coatings in cheese
855 preservation: Opportunities and challenges. *Food Research International* 107:84–92.
856 <https://doi.org/10.1016/j.foodres.2018.02.013>
- 857 de Britto D, Campana-Filho SP (2007) Kinetics of the thermal degradation of chitosan.
858 *Thermochimica Acta* 465:73–82. <https://doi.org/10.1016/j.tca.2007.09.008>
- 859 Decker EA, Welch B (1990) Role of ferritin as a lipid oxidation catalyst in muscle food. *J Agric*
860 *Food Chem* 38:674–677. <https://doi.org/10.1021/jf00093a019>
- 861 Di Pierro P, Chico B, Villalonga R, et al (2006) Chitosan–whey protein edible films produced
862 in the absence or presence of transglutaminase: analysis of their mechanical and barrier
863 properties. *Biomacromolecules* 7:744–749. <https://doi.org/10.1021/bm050661u>
- 864 Fang Y, Tung MA, Britt IJ, et al (2002) Tensile and barrier properties of edible films made
865 from whey proteins. *Journal of Food Science* 67:188–193.
866 <https://doi.org/10.1111/j.1365-2621.2002.tb11381.x>
- 867 Farajzadeh F, Motamedzadegan A, Shahidi S-A, Hamzeh S (2016) The effect of chitosan-
868 gelatin coating on the quality of shrimp (*Litopenaeus vannamei*) under refrigerated
869 condition. *Food Control* 67:163–170. <https://doi.org/10.1016/j.foodcont.2016.02.040>
- 870 Galiano F, Briceño K, Marino T, et al (2018) Advances in biopolymer-based membrane
871 preparation and applications. *Journal of Membrane Science* 564:562–586.
872 <https://doi.org/10.1016/j.memsci.2018.07.059>
- 873 Gennadios A, Handa A, Froning GW, et al (1998) Physical properties of egg white–dialdehyde
874 starch films. *J Agric Food Chem* 46:1297–1302. <https://doi.org/10.1021/jf9708047>
- 875 Gray JI, Gomaa EA, Buckley DJ (1996) Oxidative quality and shelf life of meats. *Meat Science*
876 43:111–123. [https://doi.org/10.1016/0309-1740\(96\)00059-9](https://doi.org/10.1016/0309-1740(96)00059-9)
- 877 Hajji S, Kchaou H, Bkhairia I, et al (2021) Conception of active food packaging films based on
878 crab chitosan and gelatin enriched with crustacean protein hydrolysates with improved
879 functional and biological properties. *Food Hydrocolloids* 116:106639.
880 <https://doi.org/10.1016/j.foodhyd.2021.106639>
- 881 Hajji S, Younes I, Ghorbel-Bellaaj O, et al (2014) Structural differences between chitin and
882 chitosan extracted from three different marine sources. *International Journal of*
883 *Biological Macromolecules* 65:298–306.
884 <https://doi.org/10.1016/j.ijbiomac.2014.01.045>
- 885 Hamdi M, Hajji S, Affes S, et al (2018) Development of a controlled bioconversion process for
886 the recovery of chitosan from blue crab (*Portunus segnis*) exoskeleton. *Food*
887 *Hydrocolloids* 77:534–548. <https://doi.org/10.1016/j.foodhyd.2017.10.031>
- 888 Hamdi M, Nasri R, Amor IB, et al (2020) Structural features, anti-coagulant and anti-adhesive
889 potentials of blue crab (*Portunus segnis*) chitosan derivatives: Study of the effects of

- 890 acetylation degree and molecular weight. *International Journal of Biological*
891 *Macromolecules* 160:593–601. <https://doi.org/10.1016/j.ijbiomac.2020.05.246>
- 892 Hamdi M, Nasri R, Li S, Nasri M (2019) Bioactive composite films with chitosan and
893 carotenoproteins extract from blue crab shells: Biological potential and structural,
894 thermal, and mechanical characterization. *Food Hydrocolloids* 89:802–812.
895 <https://doi.org/10.1016/j.foodhyd.2018.11.062>
- 896 Hamed I, Özogul F, Regenstein JM (2016) Industrial applications of crustacean by-products
897 (chitin, chitosan, and chitooligosaccharides): A review. *Trends in Food Science &*
898 *Technology* 48:40–50. <https://doi.org/10.1016/j.tifs.2015.11.007>
- 899 Horwitz W (2000) *Official methods of analysis of AOAC International*. AOAC International,
900 Gaithersburg, Md.
- 901 Jiang S, Zhang X, Ma Y, et al (2016) Characterization of whey protein-carboxymethylated
902 chitosan composite films with and without transglutaminase treatment. *Carbohydrate*
903 *Polymers* 153:153–159. <https://doi.org/10.1016/j.carbpol.2016.07.094>
- 904 Kaanane A, Mkaem H (2020) Valorization technologies of marine by-products. in: *innovation*
905 *in the food sector through the valorization of food and agro-food by-products*.
906 IntechOpen
- 907 Kalaycıoğlu Z, Torlak E, Akın-Evingür G, et al (2017) Antimicrobial and physical properties
908 of chitosan films incorporated with turmeric extract. *Int J Biol Macromol* 101:882–888.
909 <https://doi.org/10.1016/j.ijbiomac.2017.03.174>
- 910 Kamdem DP, Shen Z, Nabinejad O, Shu Z (2019) Development of biodegradable composite
911 chitosan-based films incorporated with xylan and carvacrol for food packaging
912 application. *Food Packaging and Shelf Life* 21:100344.
913 <https://doi.org/10.1016/j.fpsl.2019.100344>
- 914 Kaya M, Ravikumar P, İlk S, et al (2018) Production and characterization of chitosan based
915 edible films from *Berberis crataegina*'s fruit extract and seed oil. *Innovative Food*
916 *Science & Emerging Technologies* 45:287–297.
917 <https://doi.org/10.1016/j.ifset.2017.11.013>
- 918 Kchaou H, Jridi M, Abdelhedi O, et al (2017) Development and characterization of cuttlefish
919 (*Sepia officinalis*) skin gelatin-protein isolate blend films. *International Journal of*
920 *Biological Macromolecules* 105:1491–1500.
921 <https://doi.org/10.1016/j.ijbiomac.2017.06.056>
- 922 Keller JE, Skelley GC, Acton JC (1974) Effect of meat particle size and casing diameter on
923 summer sausage properties during drying1. *Journal of Milk and Food Technology*
924 37:101–106. <https://doi.org/10.4315/0022-2747-37.2.101>
- 925 Khan S, Ranjha NM (2014) Effect of degree of cross-linking on swelling and on drug release
926 of low viscous chitosan/poly(vinyl alcohol) hydrogels. *Polym Bull* 71:2133–2158.
927 <https://doi.org/10.1007/s00289-014-1178-2>

- 928 Kittur F, Kumar K, Tharanathan R (1998) Functional packaging properties of chitosan films.
 929 Zeitschrift für Lebensmittel-Untersuchung und -Forschung 206:44–47.
 930 <https://doi.org/10.1007/s002170050211>
- 931 Kortei NK, Odamtten GT, Obodai M, et al (2015) Determination of color parameters of gamma
 932 irradiated fresh and dried mushrooms during storage. BIOTECHNOLOGY AND
 933 NUTRITION 6
- 934 Li B, Shan C-L, Zhou Q, et al (2013) Synthesis, characterization, and antibacterial activity of
 935 cross-linked chitosan-glutaraldehyde. Mar Drugs 11:1534–1552.
 936 <https://doi.org/10.3390/md11051534>
- 937 Li C, Pei J, Zhu S, et al (2020) Development of chitosan/peptide films: physical, antibacterial
 938 and antioxidant properties. Coatings 10:1193.
 939 <https://doi.org/10.3390/coatings10121193>
- 940 Liu J, Wang H, Wang P, et al (2018) Films based on κ -carrageenan incorporated with curcumin
 941 for freshness monitoring. Food Hydrocolloids 83:134–142.
 942 <https://doi.org/10.1016/j.foodhyd.2018.05.012>
- 943 Lowry OH, Rosebrough NJ, Farr A, Randall RJ (1951) Protein measurement with the folin
 944 Phenol Reagent. J Biol Chemistry 193:256–275. [https://doi.org/10.1016/S0021-](https://doi.org/10.1016/S0021-9258(19)52451-6)
 945 [9258\(19\)52451-6](https://doi.org/10.1016/S0021-9258(19)52451-6)
- 946 Ma D, Jiang Y, Ahmed S, et al (2020) Antilisterial and physical properties of polysaccharide-
 947 collagen films embedded with cell-free supernatant of Lactococcus lactis. International
 948 Journal of Biological Macromolecules 145:1031–1038.
 949 <https://doi.org/10.1016/j.ijbiomac.2019.09.195>
- 950 Marshall DL, Wiese-Lehigh PL (1997) Comparison of impedance, microbial, sensory, and pH
 951 methods to determine shrimp quality. Journal of Aquatic Food Product Technology
 952 6:17–31. https://doi.org/10.1300/J030v06n02_03
- 953 Mathew S, Brahmakumar M, Abraham TE (2006) Microstructural imaging and characterization
 954 of the mechanical, chemical, thermal, and swelling properties of starch–chitosan blend
 955 films. Biopolymers 82:176–187. <https://doi.org/10.1002/bip.20480>
- 956 Matta E, Tavera-Quiroz MJ, Bertola N (2019) Active edible films of methylcellulose with
 957 extracts of green apple (Granny Smith) skin. International Journal of Biological
 958 Macromolecules 124:1292–1298. <https://doi.org/10.1016/j.ijbiomac.2018.12.114>
- 959 Melro E, Antunes FE, da Silva GJ, et al (2020) Chitosan films in food applications. tuning film
 960 properties by changing acidic dissolution conditions. Polymers 13:1.
 961 <https://doi.org/10.3390/polym13010001>
- 962 Mihalca V, Kerezsi AD, Weber A, et al (2021) Protein-based films and coatings for food
 963 industry applications. Polymers 13:769. <https://doi.org/10.3390/polym13050769>
- 964 Moalla S, Ammar I, Fauconnier M-L, et al (2021) Development and characterization of chitosan
 965 films carrying Artemisia campestris antioxidants for potential use as active food
 966 packaging materials. International Journal of Biological Macromolecules 183:254–266.
 967 <https://doi.org/10.1016/j.ijbiomac.2021.04.113>

- 968 Mohebi E, Shahbazi Y (2017) Application of chitosan and gelatin based active packaging films
 969 for peeled shrimp preservation: A novel functional wrapping design. *LWT - Food*
 970 *Science and Technology* 76:108–116. <https://doi.org/10.1016/j.lwt.2016.10.062>
- 971 Muñoz I, Rodríguez C, Gillet D, M. Moerschbacher B (2018) Life cycle assessment of chitosan
 972 production in india and europe. *Int J Life Cycle Assess* 23:1151–1160.
 973 <https://doi.org/10.1007/s11367-017-1290-2>
- 974 Na S, Kim J-H, Jang H-J, et al (2018) Shelf-life extension of Pacific white shrimp (*Litopenaeus*
 975 *vannamei*) using chitosan and ϵ -polylysine during cold storage. *Int J Biol Macromol*
 976 115:1103–1108. <https://doi.org/10.1016/j.ijbiomac.2018.04.180>
- 977 Ozogul F, Hamed I, Özogul Y, Regenstein J (2018) Crustacean By-products
- 978 Pitak N, Rakshit SK (2011) Physical and antimicrobial properties of banana flour/chitosan
 979 biodegradable and self-sealing films used for preserving Fresh-cut vegetables. *LWT -*
 980 *Food Science and Technology* 44:2310–2315.
 981 <https://doi.org/10.1016/j.lwt.2011.05.024>
- 982 Prieto P, Pineda M, Aguilar M (1999) Spectrophotometric quantitation of antioxidant capacity
 983 through the formation of a phosphomolybdenum complex: specific application to the
 984 determination of vitamin E. *Anal Biochem* 269:337–341.
 985 <https://doi.org/10.1006/abio.1999.4019>
- 986 Romadhoni AR, Afrianto E, Pratama RI, Grandiosa R (2016) Extraction of snakehead fish
 987 [*ophiocephalus striatus* (bloch, 1793)] into fish protein concentrate as albumin source
 988 using various solvent. *Aquatic Procedia* 7:4–11.
 989 <https://doi.org/10.1016/j.aqpro.2016.07.001>
- 990 Rudovica V, Rotter A, Gaudêncio SP, et al (2021) Valorization of marine waste: use of
 991 industrial by-products and beach wrack towards the production of high added-value
 992 products. *Frontiers in Marine Science* 8:
- 993 Santos VP, Marques NSS, Maia PCSV, et al (2020) Seafood waste as attractive source of chitin
 994 and chitosan production and their applications. *Int J Mol Sci* 21:4290.
 995 <https://doi.org/10.3390/ijms21124290>
- 996 Shantha NC, Decker EA (1993) Conjugated linoleic acid concentrations in processed cheese
 997 containing hydrogen donors, iron and dairy-based additives. *Food Chemistry* 47:257–
 998 261. [https://doi.org/10.1016/0308-8146\(93\)90158-C](https://doi.org/10.1016/0308-8146(93)90158-C)
- 999 Song W, Kong X, Hua Y, et al (2020) Identification of antibacterial peptides generated from
 1000 enzymatic hydrolysis of cottonseed proteins. *LWT* 125:109199.
 1001 <https://doi.org/10.1016/j.lwt.2020.109199>
- 1002 Srinivasan M, Holl FB, Petersen DJ (2011) Influence of indoleacetic-acid-producing *Bacillus*
 1003 isolates on the nodulation of *Phaseolus vulgaris* by *Rhizobium etli* under gnotobiotic
 1004 conditions. *Canadian Journal of Microbiology*. <https://doi.org/10.1139/m96-129>
- 1005 Sun L, Sun J, Chen L, et al (2017) Preparation and characterization of chitosan film
 1006 incorporated with thinned young apple polyphenols as an active packaging material.
 1007 *Carbohydrate Polymers* 163:81–91. <https://doi.org/10.1016/j.carbpol.2017.01.016>

- 1008 Valdivia-López MA, Tecante A, Granados-Navarrete S, Martínez-García C (2016) Preparation
1009 of modified films with protein from grouper fish. *International Journal of Food Science*
1010 2016:1–9. <https://doi.org/10.1155/2016/3926847>
- 1011 W. Apriliyani M, Purwadi P, Manab A, et al (2020) Characteristics of moisture content,
1012 swelling, opacity and transparency with addition chitosan as edible films/coating base
1013 on casein. *AJFST* 18:9–14. <https://doi.org/10.19026/ajfst.18.6041>
- 1014 Wang L, Ding J, Fang Y, et al (2020) Effect of ultrasonic power on properties of edible
1015 composite films based on rice protein hydrolysates and chitosan. *Ultrasonics*
1016 *Sonochemistry* 65:105049. <https://doi.org/10.1016/j.ultsonch.2020.105049>
- 1017 Xiong Y, Chen M, Warner RD, Fang Z (2020) Incorporating nisin and grape seed extract in
1018 chitosan-gelatine edible coating and its effect on cold storage of fresh pork. *Food*
1019 *Control* 110:107018. <https://doi.org/10.1016/j.foodcont.2019.107018>
- 1020 Yildirim A, Mavi A, Kara AA (2001) Determination of antioxidant and antimicrobial activities
1021 of *Rumex crispus* L. extracts. *J Agric Food Chem* 49:4083–4089.
1022 <https://doi.org/10.1021/jf0103572>
- 1023 Yuan Y, Zhang X, Pan Z, et al (2021) Improving the properties of chitosan films by
1024 incorporating shellac nanoparticles. *Food Hydrocolloids* 110:106164.
1025 <https://doi.org/10.1016/j.foodhyd.2020.106164>
- 1026 Zhang L, Liu Z, Wang X, et al (2019a) The properties of chitosan/zein blend film and effect of
1027 film on quality of mushroom (*Agaricus bisporus*). *Postharvest Biology and Technology*
1028 155:47–56. <https://doi.org/10.1016/j.postharvbio.2019.05.013>
- 1029 Zhang L, Liu Z, Wang X, et al (2019b) The properties of chitosan/zein blend film and effect of
1030 film on quality of mushroom (*Agaricus bisporus*). *Postharvest Biology and Technology*
1031 155:47–56. <https://doi.org/10.1016/j.postharvbio.2019.05.013>
- 1032 Zhang X, Lian H, Shi J, et al (2020) Plant extracts such as pine nut shell, peanut shell and jujube
1033 leaf improved the antioxidant ability and gas permeability of chitosan films.
1034 *International Journal of Biological Macromolecules* 148:1242–1250.
1035 <https://doi.org/10.1016/j.ijbiomac.2019.11.108>
- 1036
- 1037